Quantum spin liquid phases in the bilinear-biquadratic two-SU(4)-fermion Hamiltonian on the square lattice

Olivier Gauthé [1,2] Sylvain Capponi [1] Matthieu Mambrini,[1] and Didier Poilblanc[1,2]

[1]*Laboratoire de Physique Théorique, Université de Toulouse, CNRS, UPS, France*
[2]*Institute of Theoretical Physics, École Polytechnique Fédérale de Lausanne (EPFL), CH-1015 Lausanne, Switzerland*

We consider the phase diagram of the most general SU(4)-symmetric two-site Hamiltonian for a system of two fermions per site (i.e., self-conjugate **6** representation) on the square lattice. It is known that this model hosts magnetic phases breaking SU(4) symmetry and quantum disordered dimerlike phases breaking lattice translation symmetry. Motivated by a previous work [O. Gauthé, S. Capponi, and D. Poilblanc, Phys. Rev. B **99**, 241112(R) (2019)], we investigate the possibility of the existence of SU(4) quantum spin liquid phases in this model, using SU(4)-symmetric projected entangled pair states (PEPS) of small bond dimensions, which can be classified according to point group and charge (C) symmetries. Among several (disconnected) families of SU(4)-symmetric PEPS, breaking or not C-symmetry, we identify critical or topological spin liquids which may be stable in some regions of the phase diagram. These results are confronted to exact diagonalization (ED) and density matrix renormalization group (DMRG) calculations.

I. INTRODUCTION

With the realization of ultracold gases of atoms with N internal (nucleus) degrees of freedom loaded on periodic optical lattices [1,2], an interest is rapidly growing for spin Hamiltonians with exact SU(N) symmetry. Various lattices, SU(N) symmetries and SU(N) irreducible representations (irreps) have been studied [3–8], showing a plethora of novel phases, most of them spontaneously breaking lattice or SU(N) symmetries, like valence bond crystals (VBC) or magnetic states. However, a few studies were devoted to the explicit construction of SU(N) quantum spin liquids (QSL) preserving both SU(N) and lattice symmetries [9–11]. Tensor networks like Projected Entangled Pair States (PEPS) are particularly well suited to the construction of QSL states. For example, a previous work proposed critical QSL and a $\mathbb{Z}_2$ topological QSL phase for a system of two SU(4) fermions per site. Although VBC are ubiquitous in the study of SU(N)-invariant models, (nonchiral) spin liquids seem to be relatively rare. Here we revisit a SU(4)-symmetric bilinear-biquadratic Hamiltonian with two fermions in the self-conjugate **6**-irrep of SU(4) on each site [12–14]. Using exact diagonalization (ED), density matrix renormalization group (DMRG), and infinite-PEPS (iPEPS) numerical methods, we identify two different types of SU(4) spin liquids which appear to be very competitive in energy in two regions of the (one parameter) phase diagram.

II. MODEL AND HAMILTONIAN

We consider a square lattice where we attach a SU(4) irreducible representation $\mathbf{6} \equiv \square$ corresponding to the six antisymmetric states of two SU(4) (atomic) fermions on each site. We also assume a coupling between nearest-neighbor

(NN) sites only. Starting from the fusion rule on two sites,

$$\square \otimes \square = \bullet \oplus \overset{\square}{\square} \oplus \square\square, \qquad (1)$$

we see that three SU(4) symmetric projectors can be defined on these two sites: $\mathcal{P}_\mathbf{1}$, $\mathcal{P}_\mathbf{15}$, and $\mathcal{P}_\mathbf{20'}$, corresponding to the fusion outcomes characterized by the irreps **1**, **15**, and **20'**, on the right-hand side of Eq. (1), respectively. One can use the projectors $\mathcal{P}_\alpha$ as a natural basis to expand the Hamiltonian $\mathcal{H} = \sum_\alpha c_\alpha \mathcal{P}_\alpha$, $c_\alpha \in \mathbb{R}$. The operator $\mathbf{S} \cdot \mathbf{S}$ on two sites writes $\mathbf{S} \cdot \mathbf{S} = -5\mathcal{P}_\mathbf{1} - \mathcal{P}_\mathbf{15} + \mathcal{P}_\mathbf{20'}$, which, as can be seen straightforwardly, is linearly independent from $(\mathbf{S} \cdot \mathbf{S})^2 = 25\mathcal{P}_\mathbf{1} + \mathcal{P}_\mathbf{15} + \mathcal{P}_\mathbf{20'}$. As $\sum_\alpha \mathcal{P}_\alpha = \mathcal{I}_d$, the most general two-site SU(4) symmetric (real) Hamiltonian can then be re-expressed as a linear combination of $\mathbf{S} \cdot \mathbf{S}$ and $(\mathbf{S} \cdot \mathbf{S})^2$ (up to a constant energy shift) and can be parametrized by a single parameter θ. Following the conventions of Ref. [15], the lattice Hamiltonian becomes

$$\mathcal{H}(\theta) = \cos\theta \sum_{\langle ij \rangle} \mathbf{S}_i \cdot \mathbf{S}_j + \frac{\sin\theta}{4} \sum_{\langle ij \rangle} (\mathbf{S}_i \cdot \mathbf{S}_j)^2, \qquad (2)$$

where the sum is restricted to nearest-neighbor bonds $\langle ij \rangle$. In addition to the invariance with respect to (w.r.t.) the lattice symmetries and the SU(4) spin symmetry, Hamiltonian Eq. (2) is also invariant w.r.t. color (or "charge") conjugation (C) since physical degrees of freedom correspond to a self-conjugate irrep of SU(4).

Importantly, there are four SU(6) points, when the coefficients in front of two projectors are identical, and the fusion rules are enhanced to that of SU(6): (i) at $\theta = \pi/4$ and $\theta = -3\pi/4$, the fusion rule is enhanced to $\mathbf{6} \otimes \mathbf{6} = \mathbf{15} \oplus \mathbf{21}$ and

(ii) at $\theta = \pm\pi/2$, the fusion rule becomes $\mathbf{6} \otimes \bar{\mathbf{6}} = \mathbf{1} \oplus \mathbf{35}$. The corresponding NN bond operators of the Hamiltonian read

$$\mathcal{H}_{\mathbf{6}\bar{\mathbf{6}}}^{b} = \mp\left(\frac{25}{4}\mathcal{P}_{\mathbf{1}} + \frac{1}{4}\mathcal{P}_{\mathbf{15}\oplus\mathbf{20'}}\right) = \mp\left(6\mathcal{P}_{\mathbf{1}} + \frac{1}{4}\mathbb{1}\right), \quad (3)$$

$$\mathcal{H}_{\mathbf{66}}^{b} = \mp\frac{\sqrt{2}}{2}\left(\frac{3}{4}\mathcal{P}_{\mathbf{15}} - \frac{5}{4}\mathcal{P}_{\mathbf{20'}\oplus\mathbf{1}}\right) = \mp\frac{\sqrt{2}}{2}\left(2\mathcal{P}_{\mathbf{15}} - \frac{5}{4}\mathbb{1}\right) \quad (4)$$

$$= \pm\frac{\sqrt{2}}{2}\left(\mathbb{P}_{\text{SU}(6)} + \frac{1}{4}\mathbb{1}\right), \quad (5)$$

where the $-$ and $+$ signs in Eqs. (3) and (4) correspond to the antiferromagnetic (AF) and ferromagnetic (F) couplings, respectively. The two-site SU(4) Hilbert spaces spanned by **15**, $\mathbf{15} \oplus \mathbf{20'}$, and $\mathbf{20'} \oplus \mathbf{1}$ can be mapped on the spaces spanned by **15**, **35**, and **21** of SU(6), respectively. Equations (3) and (4) are defined in terms of the alternating and uniform fundamental representation $\square$ of SU(6), respectively. In the following, we shall refer to these enhanced symmetry points as SU(6) $\mathbf{6}\bar{\mathbf{6}}$ and SU(6) $\mathbf{66}$ symmetric points. At the latter higher symmetry point, the bond operator can be written in terms of the SU(6) color permutation $\mathbb{P}_{\text{SU}(6)}$, as shown in Eq. (5).

III. CRITICAL DISCUSSION OF THE PHASE DIAGRAM

In this section we discuss the current understanding of the model. We start by drawing a tentative phase diagram based on the work by Paramekanti *et al.* [16]. We then discuss our ED studies that bring new insights, still leaving a number of open issues.

A pure bilinear model $\theta = 0$ is expected to stabilize an ordered antiferromagnetic (Néel) phase that breaks SU(4) symmetry [13], similarly to SU(2) antiferromagnetic Heisenberg models. Similarly, a ferromagnetic phase is expected in the vicinity of the ferromagnetic Heisenberg point at $\theta = \pm\pi$. We build our work starting from early calculations based on projected wave functions [16]. A schematic phase diagram based on this approach is shown in Fig. 1(a). Interestingly, besides the expected magnetic phases mentioned above, their phase diagram shows SU(4)-invariant quantum disordered (QD) phases, a dimerized phase and a C-breaking phase. It also suggests the existence of a third QD phase in a narrow region around $\theta = 0.19\pi$ (thus, for a sign of the biquadratic interaction appropriate to a half-filled fermionic SU(4) Hubbard model [17]), which they attribute to a gapless staggered flux state [15].

We have tried to refine the phase diagram using ED of four periodic $N = 8, 10, 12, 16$ square clusters; see Appendix B. Note that these clusters unfortunately, have different lattice symmetries: for instance, reflection symmetry is missing in the 10- and 12-site cluster, the 16-site clusters can be mapped on a four-dimensional cube with larger symmetry, and the reciprocal space of the 10- and 12-site clusters does not contain the $\mathbf{q}_{\text{VBC}} = (\pi, 0)$ wave vector. However, all clusters show consistently the existence of two first order transitions characterized by the simultaneous crossing of many nonsinglet SU(4) states [including the highest-weight multiplet of SU(4)] with a SU(4) singlet state, and occurring at exactly the
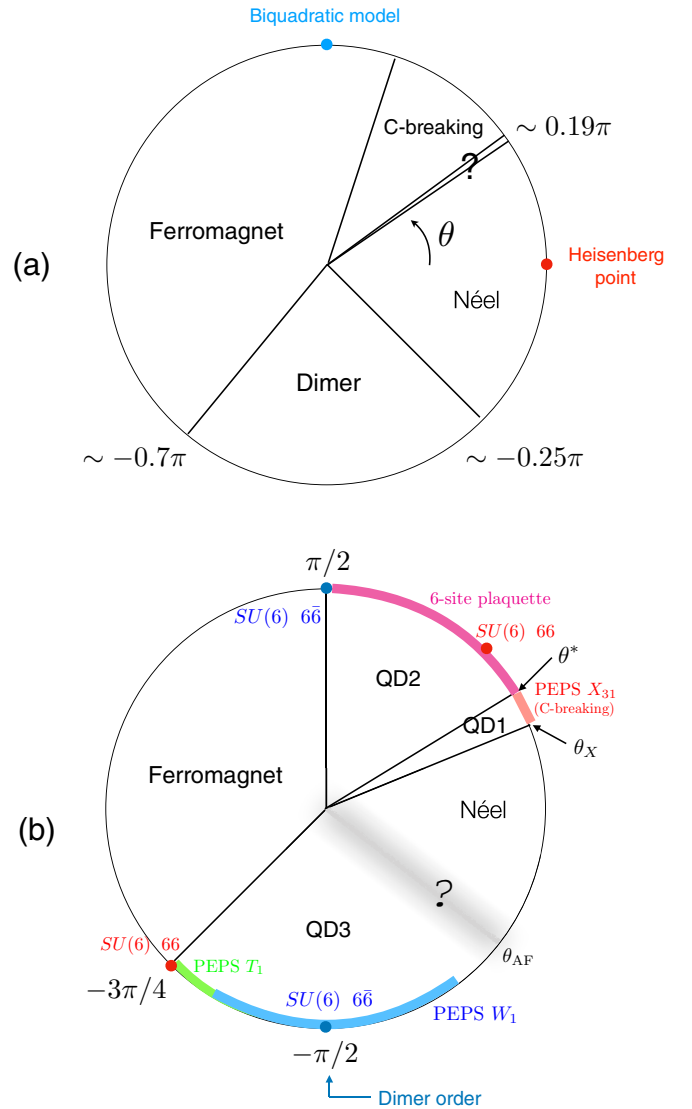

FIG. 1. Tentative phase diagrams as a function of θ. (a) Adaptation from Ref. [16]. Antiferromagnet and ferromagnetic orders are expected in some region around the antiferromagnetic and the ferromagnetic ($\theta = \pi$) points. A dimer phase (or more generally a VBC phase) is expected around $\theta = -\pi/2$. A C-breaking phase as well as a staggered flux state (indicated by a question mark) have been also proposed. (b) Phase diagram drawn from ED results on periodic clusters (see text). The ferromagnetic phase is limited by first-order transitions exactly at the SU(6)-symmetric points at $\theta = -3\pi/4$ and $\theta = \pi/2$ (showing massive level crossings on all finite clusters). We have identified three quantum disordered (QD) regions from low-energy singlet excitations and marked the regions where the PEPS QSL constructed in this work may be relevant. The variational [SU(6)-symmetric] six-site plaquette phase is also shown.

SU(6)-symmetric points $\theta = -3\pi/4$ and $\theta = \pi/2$, as shown in Figs. 2(a) and 5(a). At these two crossings we have checked that the ground state correspond exactly to the SU(6) irrep of largest weight, i.e., to the SU(6) ferromagnet. These points hence mark the exact boundaries of the ferromagnetic phase as represented in the new phase diagram on Fig. 1(b). The
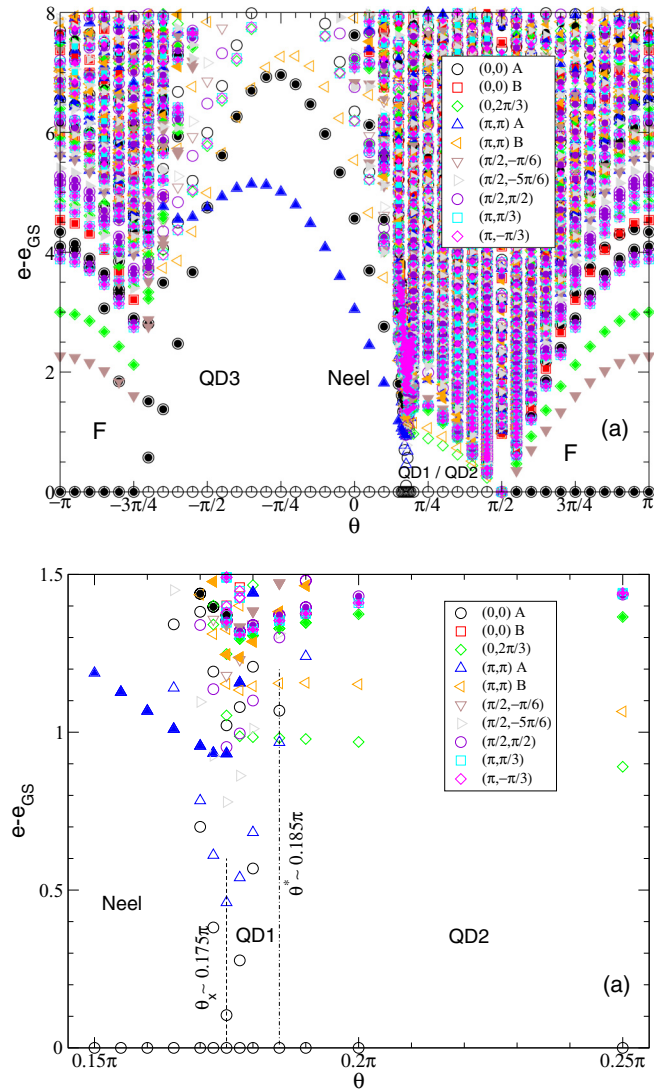
FIG. 2. ED energy spectrum of the periodic 12-site cluster. Open (closed) symbols correspond to singlets (higher dimensional irreps). Different symbols are used for different momenta in the reciprocal space. (a) Full parameter range $-\pi \leqslant \theta \leqslant \pi$. (b) Zoom of the range $0.15\pi \leqslant \theta \leqslant 0.25\pi$. Crossing of ground-state levels is observed at $\theta_X \sim 0.175\pi$, signaling a first order transition. Level crossings of (singlet) excited states at θ^* are marked by a dashed line.

existence of a magnetic Néel phase is reflected by a $\mathbf{q} = (\pi, \pi)$ magnetic low-energy excited state (i.e., belonging to a finite dimensional irrep) above the singlet GS. Due to finite-size effects, its precise boundary on one side is not fully accurate, as indicated by a question mark in Fig. 1(b). On the other side, we think it is limited by a very sharp level anti-crossing at $\theta_X \sim 0.175\pi$ as shown in Fig. 2(b) and more clearly in Fig. 5(c). In all clusters, we see a narrow region around $\theta_X < \theta < \theta^* \sim 0.185\pi$ characterized by a few low-energy singlets with different momenta [see Fig. 2(b)]—named QD1 in Fig. 1(b)—that may be consistent with a QSL like, e.g., the gapless staggered flux state or a C-breaking phase [15]. The two phases at the boundary of the ferromagnetic region are more difficult to characterize. The 12-site cluster suggests

the existence of two quantum disordered phases—named QD2 and QD3 in Fig. 1(b)—as signalled by a singlet GS with low-energy singlet excitation(s). In fact, $\theta = -\pi/2$ corresponds to the SU(6) $\mathbf{6\bar{6}}$ (antiferromagnetic) Heisenberg point whose GS is known to be dimerized, although with a quite small order parameter [18]. At the SU(6) $\mathbf{66}$ (antiferromagnetic) Heisenberg point at $\theta = \pi/4$ the ground state is always a non degenerate SU(6) singlet on clusters whose number of sites is multiple of 6.

The topological PEPS of Ref. [19] is a priori a good candidate for QD phases, but other alternatives exist. In fact, it has been proposed that the QD2 phase spontaneously breaks C-symmetry in contrast to the PEPS ansatz of Ref. [19]. This has motivated us to construct other PEPS family allowing or not for spontaneous C-breaking. The existence of SU(6)-symmetric points in the one-dimensional (1D) parameter space is also greatly constraining the PEPS family by allowing it to be fine tuned to these higher symmetries. Using iPEPS techniques we have investigated the relevance of our PEPS spin liquids in some separate regions of the phase diagram [see Fig. 1(b)]. Note that Lieb-Schultz-Mattis-Affleck theorem is likely to apply for the $\square$ irrep of SU(6) or the $\boxminus$ irrep of SU(4), corresponding to 1/6 and 1/2 fermionic filling, respectively. SU(6) and SU(4) spin liquids are therefore expected to be topological—with sixfold and (at least) twofold degenerate groundstates, respectively—or critical.

IV. SU(4)-SYMMETRIC PEPS FAMILIES

A. Simple SU(4)-symmetric PEPS

We aim here to construct simple PEPS ansatz on the square lattice which are fully invariant under SU(4) symmetry (i.e., the state is a global SU(4) singlet) and under all lattice symmetries (including lattice translations). Our PEPS are defined by a single-site rank-5 tensor with four virtual indices on the $z = 4$ bonds connecting the site to its neighbors and one index labeling the $d = 6$ states of the physical $\boxminus$ irrep as shown in Fig. 3(a). The PEPS wave function is obtained by contracting the network of tensors on the virtual indices [20].

To construct SU(4)-symmetric PEPS we follow here the framework developed in Ref. [21]. First, to enforce the invariance of the PEPS wave functions under 90-degrees rotation w.r.t. to any lattice site, the tensors should belong to the same one-dimensional irrep of the point group C_{4v}, namely, either to the rotation-even $\mathcal{A}_1$ or $\mathcal{A}_2$ irreps or to the rotation-odd $\mathcal{B}_1$ or $\mathcal{B}_2$ irreps, where the subscripts 1 and 2 refer to even and odd characters w.r.t. axis reflections, respectively. We shall not consider here the two-dimensional $\mathcal{E}$ irrep of C_{4v}. Hence, here after, we shall assume that the tensors belong to one of the four irreps of the point group, even if not explicitly specified. Second, to guarantee (global) spin-rotation invariance, the virtual space $\mathcal{V}$ has to be a direct sum of SU(4) irreps (named "species" or "particles") in such a way that the expansion of $\mathcal{V}^{\otimes z}$ in terms of SU(4) irreps contains the physical irrep $\boxminus$, possibly with some multiplicity. Restricting first to the smallest dimension $D = \dim(\mathcal{V})$, we are
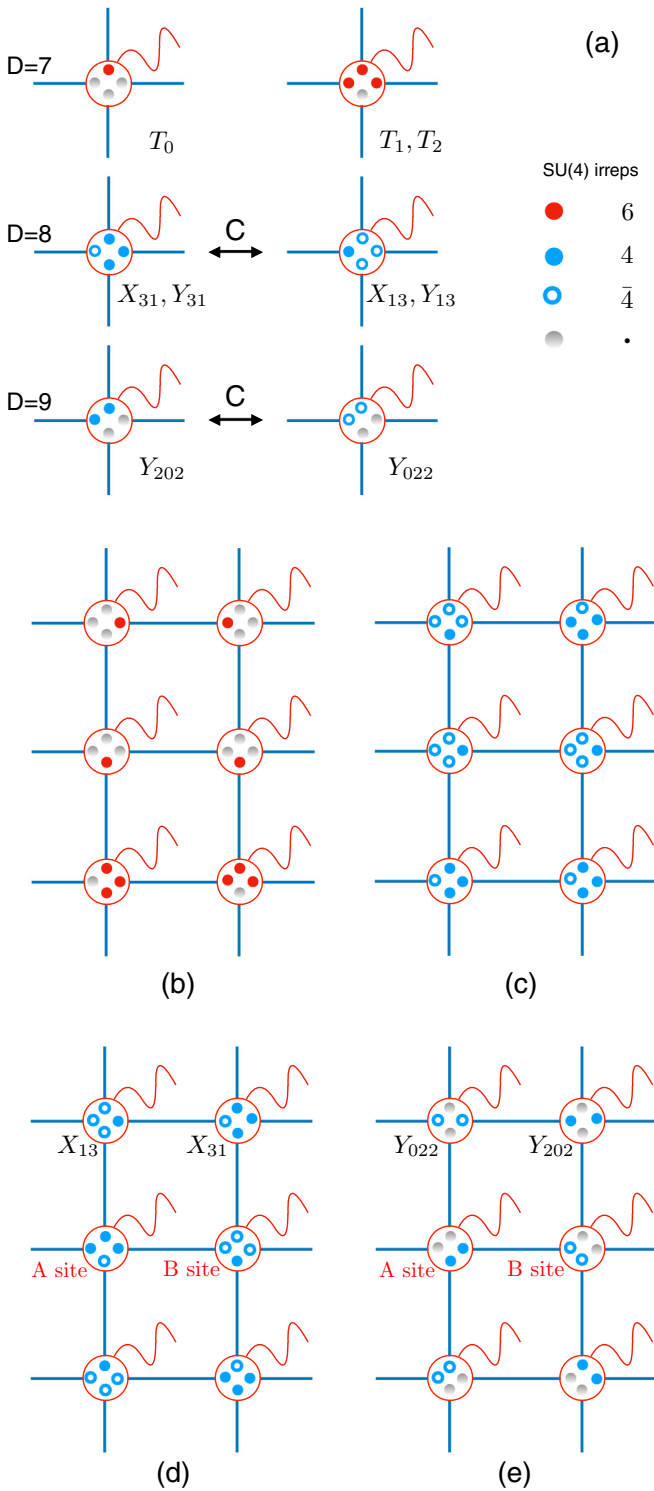
FIG. 3. (a) The smallest D SU(4)-symmetric tensors. The four virtual states (small dots) are projected (red circle) onto the physical **6** irrep (wingly line). C-conjugated pairs of tensors are indicated by the arrows. (b) A typical PEPS configuration constructed from T tensors with either •• or 66 virtual singlet bonds. (c) A typical PEPS configuration constructed with $4\bar{4}$ or $\bar{4}4$ virtual singlet bonds. (d), (e) Typical PEPS configurations of C-breaking phases with a staggered arrangement of charge conjugated tensors. In panels (b), (c), (d), and (e), the matrices located on the bond centers that enforce the projections on SU(4) singlets are omitted for clarity.

left with

$$\mathcal{V} = \square \oplus \bullet \equiv \mathbf{6} \oplus \mathbf{1}, \tag{6}$$

$$\mathcal{V} = \square \oplus \begin{matrix}\square\\\square\end{matrix} \equiv \mathbf{4} \oplus \bar{\mathbf{4}}, \tag{7}$$

$$\mathcal{V} = \square \oplus \begin{matrix}\square\\\square\end{matrix} \oplus \bullet \equiv \mathbf{4} \oplus \bar{\mathbf{4}} \oplus \mathbf{1}, \tag{8}$$

with bond dimension $D = 7$, $D = 8$, and $D = 9$, respectively. The different classes of tensors are shown in Fig. 3(a).

Note that the $D = 8$ tensors are just a subset of the set of $D = 9$ tensors. Both $D = 7$ and $D = 8$ tensors have a $\mathbb{Z}_2$ *gauge* (i.e., connected to the virtual space only) symmetry since each of the two species entering $\mathcal{V}$ appears an odd number of times (one or three times) on the four tensor *virtual* legs. Importantly, we note in Eqs. (7) and (8) the emergence of a charge conjugation symmetry C exchanging $\mathbf{4} \leftrightarrow \bar{\mathbf{4}}$ and leaving the physical space **6** invariant. Note that unlike the SU(2) case, SU(4) charge conjugation is not a group operation. PEPS associated to the tensors with, e.g., virtual space Eqs. (6) and (7) can be constructed by contracting over the virtual indices, as shown in Figs. 3(b) and 3(c), respectively.

Let us first look more closely at the $D = 7$ PEPS family: its generic on-site tensor A_T is given by a linear combination of three (real) $D = 7$ tensors T_0, T_1, and T_2 given in Ref. [19],

$$A_T = a_0 T_0 + a_1 T_1 + a_2 T_2, \tag{9}$$

with $a_i \in \mathbb{R}$ and a_0 can be fixed to 1. These tensors are real and invariant under all symmetry operations of the lattice point group (i.e., the C_{4v} group)—namely, they belong to the $\mathcal{A}_1$ representation of the group—so that all PEPS of the family preserve parity (P) symmetry. The tensors can be labeled by an "occupation number" n_{occ} specifying, for each species in the virtual space, its total number on the four legs. For example, for T_0, for which one has two different species **6** and **1**, $n_{\text{occ}} = \{1, 3\}$. For T_1 and T_2, $n_{\text{occ}} = \{3, 1\}$. Properties of the T tensors are summarized in Table I. Note that the tensor T_0 alone generates the nearest-neighbor SU(4) Resonating Valence Bond (RVB) state [19]. Note also that it is also possible to add a pure imaginary tensor $ia_3 T_3$ to (9), breaking time-reversal symmetry (T), while preserving all lattice symmetries.

Tensors with virtual space $\mathbf{4} \oplus \bar{\mathbf{4}}$ can also be classified according to their point group symmetry. As shown in Table I, one (two) pair(s) of C-conjugated X_{13} and X_{31} ($Y_{13}^{(i)}$ and $Y_{31}^{(i)}$, $i = 1, 2$) tensors have $\mathcal{A}_1$ ($\mathcal{A}_2$) symmetry. A general PEPS ansatz preserving C_{4v} symmetry can be obtained from a local tensor combining all X tensors in the following way:

$$A_X = A_R + iA_I, \quad A_R = X_{31} + \alpha X_{13},$$
$$A_I = \sum_i \left(\beta_{31}^{(i)} Y_{31}^{(i)} + \beta_{13}^{(i)} Y_{13}^{(i)} \right), \tag{10}$$

where $A_I \neq 0$ would spontaneously break time-reversal symmetry. Similarly, one can use the Y_{202} and Y_{022} tensors (of $\mathcal{A}_2$ point group symmetry) which include an extra spin singlet in

TABLE I. Classification of $\mathbf{6} \oplus \mathbf{1}$ and $\mathbf{4} \oplus \overline{\mathbf{4}}$ SU(4)-symmetric tensors in terms of virtual space, action of SU(4) charge conjugation (C) and C_{4v} irreps. Tensors T_0, T_1, and W_1 are more symmetric and are invariant under any virtual leg permutation. The occupation numbers of each virtual species on the four virtual bonds are shown within brackets.

A	D	$\mathcal{V}$	n_{occ}	C	C_{4v}
T_0	7	$\mathbf{6} \oplus \mathbf{1}$	1,3	✓	$\mathcal{A}_1$
T_1	7	$\mathbf{6} \oplus \mathbf{1}$	3,1	✓	$\mathcal{A}_1$
T_2	7	$\mathbf{6} \oplus \mathbf{1}$	3,1	✓	$\mathcal{A}_1$
T_3	7	$\mathbf{6} \oplus \mathbf{1}$	3,1	✓	$\mathcal{A}_2$
X_{31}	8	$\mathbf{4} \oplus \overline{\mathbf{4}}$	3,1	✗	$\mathcal{A}_1$
$Y_{31}^{(i)}$	8	$\mathbf{4} \oplus \overline{\mathbf{4}}$	3,1	✗	$\mathcal{A}_2$
X_{13}	8	$\mathbf{4} \oplus \overline{\mathbf{4}}$	1,3	✗	$\mathcal{A}_1$
$Y_{13}^{(i)}$	8	$\mathbf{4} \oplus \overline{\mathbf{4}}$	1,3	✗	$\mathcal{A}_2$
Y_{202}	9	$\mathbf{4} \oplus \overline{\mathbf{4}} \oplus \mathbf{1}$	{2, 0, 2}	✗	$\mathcal{A}_2$
Y_{022}	9	$\mathbf{4} \oplus \overline{\mathbf{4}} \oplus \mathbf{1}$	{0, 2, 2}	✗	$\mathcal{A}_2$
$W_{(i)}$	13	$\mathbf{6} \oplus \mathbf{6} \oplus \mathbf{1}$	{2, 1, 1}	✓	$\mathcal{A}_1$

the virtual space,

$$A_Y = Y_{202} + \gamma Y_{022}.$$

In general, A_X (A_Y) breaks charge conjugation except when $\alpha = \pm 1$ and $\beta_{31}^{(i)} = \pm \beta_{13}^{(i)}$ ($\gamma = \pm 1$).

In the following we shall use charge-conjugated tensors, A_X and $\overline{A_X}$ (respectively, A_Y and $\overline{A_Y}$) on the two A and B sublattices. Configurations of such states for $A_I = 0$ and $\alpha = 0$ (respectively, $\gamma = 0$) are shown in Fig. 3(d) [respectively, Fig. 3(e)]. In that case, by acting with charge conjugation on the (physical) B sites, one can rewrite the PEPS in terms of a unique A_X (or A_Y) tensor on all sites. While the tensor network is translation invariant, it must be emphasized that it is the common PEPS representation of two different wave functions that are only invariant under a translation by *two* sites (the translation by a lattice unit vector being equivalent to the conjugation of the whole lattice). These wave functions are orthogonal as their odd and even combinations are eigenvectors of the unitary charge conjugation operator with different eigenvalues. A local order parameter for translation and charge conjugation breaking can be constructed [16]. Note that closely related (but nonequivalent) ansatz can also be constructed using the *same* tensors A_X or A_Y on *both* sublattices but replacing the bond singlet projectors by singlet projectors involving the 8 virtual particles around each site of a given sublattice (so-called projected entangled simplex states or PESS), following closely the original construction by Affleck *et al.* [15].

Note that all these T, X, and Y tensors, taken individually, have an extended U(1) gauge symmetry so it is expected that their associated PEPS would have critical correlations. In fact, as can be seen in Figs. 3(d) and 3(e), resonances between configurations is obtained by on-site permutations of virtual states along closed loops, and the PEPS inherits its critical nature from that of quantum loop models on bipartite lattices [22]. Combining tensors with different n_{occ} lead to a lower $\mathbb{Z}_2$ gauge symmetry (see Appendix D).

Next, we turn to the extension of these tensors so that they can accommodate the emergent higher SU(6) symmetry present at isolated points of the phase diagram. This brings severe constraints on the tensor construction and on the form of the virtual space. In fact, we readily see that the tensors Eqs. (7) and (8) should be excluded since there is no four-dimensional irrep in SU(6) to map into. Below we shall restrict to the $\mathbf{6}\overline{\mathbf{6}}$ SU(6) symmetry, while the more involved case of the $\mathbf{66}$ symmetry is left for the Appendix.

B. PEPS with higher $\mathbf{6}\overline{\mathbf{6}}$ SU(6) symmetry

At $\theta = -\pi/2$, we know from previous ED that the GS is a nondegenerate SU(6) singlet. It is therefore legitimate to try to enlarge the SU(4)-symmetric PEPS family to capture the higher SU(6) $\mathbf{6}\overline{\mathbf{6}}$ symmetry of the model at this fine-tuned point. In fact, enforcing the enlarged symmetry leads to strong restriction on the site tensor. First, we note that the T_0 tensor alone has SU(6) symmetry and the associated SU(4) RVB PEPS is in fact a SU(6) $\mathbf{6}\overline{\mathbf{6}}$ RVB state, i.e., in the alternating fundamental irrep of SU(6). Therefore, we expect this PEPS should already give a reasonable approximate description of the GS at, or in the vicinity of, the *antiferro-magnetic* SU(6) $\mathbf{6}\overline{\mathbf{6}}$ point at $\theta = -\pi/2$, as we shall discuss below.

To enlarge the PEPS family beyond T_0, we shall require that the SU(4) tensors originate from a mapping of tensors (i) which are SU(6) symmetric and (ii) whose virtual space should only contain self-conjugate irreps or pairs of conjugate irreps of SU(6) (to be able to form virtual SU(6) singlets on the bonds). The smallest possible SU(6) virtual space $\mathcal{V}_6$ could therefore be

$$\mathcal{V}_6 = \square \oplus \begin{array}{c}\square\\\square\\\square\\\square\\\square\end{array} \oplus \bullet \equiv \mathbf{6} \oplus \overline{\mathbf{6}} \oplus \mathbf{1}, \qquad (11)$$

of dimension $D = 13$. The corresponding PEPS tensors represent the 28 SU(6) fusion channels $\mathbf{6} \otimes \mathbf{6} \otimes \overline{\mathbf{6}} \otimes \mathbf{1} \to \mathbf{6}$, of the four virtual states onto the physical state. Mapping to SU(4) would require a virtual space with irreps of the same dimensions,

$$\mathcal{V} = \square \oplus \begin{array}{c}\square\\\square\end{array} \oplus \bullet \equiv \mathbf{6} \oplus \mathbf{6}^* \oplus \mathbf{1}, \qquad (12)$$

where the $\mathbf{6}$ (self-conjugate) irrep occurs with multiplicity 2, i.e., with two "colors." Then, SU(6) charge conjugation C in Eq. (10) naturally translates here into color exchange $\mathcal{C}$, which can be viewed as an element of the SU(2)-color gauge symmetry. Note that it is convenient to use the conjugate $\mathbf{6}^*$ irrep of SU(4) (equivalent to $\mathbf{6}$ up to a basis change) which naturally maps onto the $\overline{\mathbf{6}}$ irrep of SU(6). At the higher symmetry point, the tensors on the A and B sites are related by charge/color conjugation C/$\mathcal{C}$. Hence, they have occupation numbers w.r.t. the $\mathbf{6}$, $\overline{\mathbf{6}}/\mathbf{6}^*$ and $\mathbf{1}$ species, $n_{\mathrm{occ}} = \{1, 0, 3\}$ (T_0) or $n_{\mathrm{occ}} = \{2, 1, 1\}$ (W) on the A sites, and $n_{\mathrm{occ}} = \{0, 1, 3\}$ ($\overline{T_0}/T_0^*$) or $n_{\mathrm{occ}} = \{1, 2, 1\}$ ($\overline{W}/W^*$) on the B sites. Later on, we shall consider the three W tensors, W_1, $W2$ and W_3, of
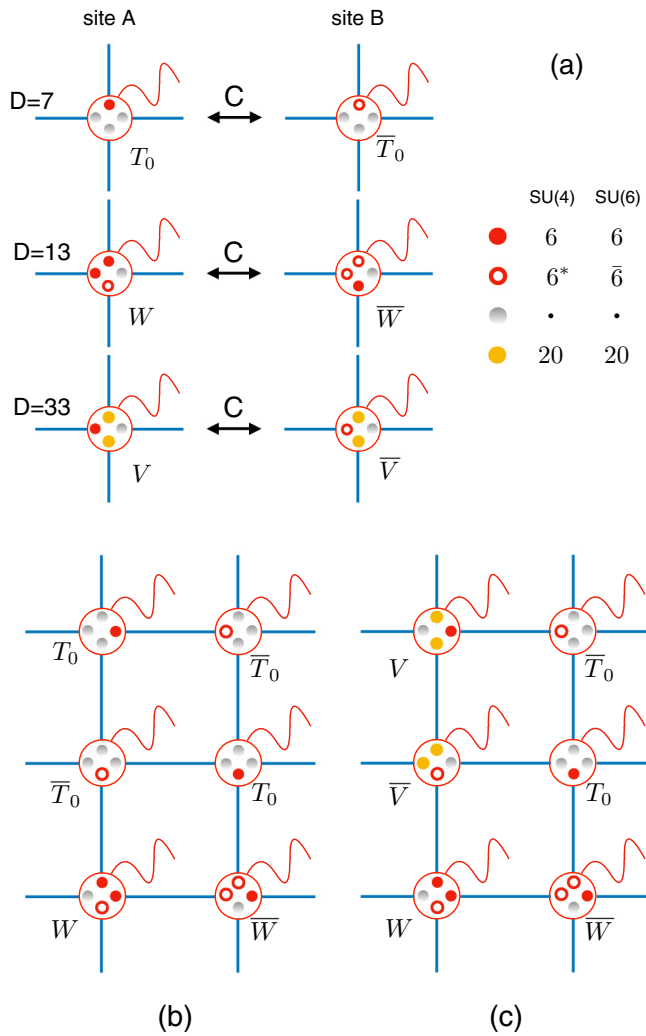
FIG. 4. (a) Three classes of SU(4) tensors with virtual spaces $\mathbf{6} \oplus \mathbf{1}$, $\mathbf{6} \oplus \mathbf{6} \oplus \mathbf{1}$, and $\mathbf{6} \oplus \mathbf{6} \oplus \mathbf{20} \oplus \mathbf{1}$ tensors, which can be mapped onto SU(6)-symmetric tensors—see Tables II and III. Color-conjugated tensors have to be used on the A and B sites to encode the $\mathbf{6\bar{6}}$ SU(6) symmetry. A uniform SU(4) PEPS ansatz is obtained by performing a basis change on the (physical) B sites. (b) Configuration of a $\mathbf{6\bar{6}}$ SU(6)-symmetric $D = 13$ PEPS. A simpler PEPS involving only the $D = 7$ tensors can be also constructed as shown on the four top sites. (c) Configuration of a $\mathbf{6\bar{6}}$ SU(6)-symmetric $D = 33$ PEPS.

$\mathcal{A}_1$ symmetry. Similarly to the tensors T_0 and T_1, the tensor W_1 is invariant under any virtual leg permutation and has an extended S_4 symmetry.

The SU(6)-symmetric PEPS is obtained by contracting the A and B tensors on all lattice bonds, as shown in Figs. 4(b) and 4(c). It is invariant under the combined action of C/$\mathcal{C}$ with a unit lattice translation. Hence, by acting with C/$\mathcal{C}$ on the (physical) B sites, one can rewrite the PEPS in terms of a unique tensor on all sites, making translation symmetry explicit.

One can even extend further the construction of the SU(6)-symmetric spin liquid by adding more irreps to the virtual space. The next step would be to include the self-conjugate [both in SU(4) and SU(6)] 20-dimensional irrep, giving

TABLE II. Full list of the classes of $D = 33$ $\mathbf{6} \oplus \mathbf{6} \oplus \mathbf{20} \oplus \mathbf{1}$ SU(4) symmetric tensors in terms of the occupation numbers of the four virtual particles. The second (third) column shows the number of SU(4) [SU(6)] fusion channels—i.e., the total number of symmetric tensors (that could be further classified in terms of the irreps of the C_{4v} point group, $\mathcal{A}_1$, $\mathcal{A}_2$, $\mathcal{B}_1$, $\mathcal{B}_2$, and $\mathcal{E}$). The $\mathbf{6} \oplus \mathbf{1}$ $\mathbf{T_0}$ (T_1, T_2) tensor(s) is (are) marked in red (brown). The other $\mathbf{6} \oplus \mathbf{6} \oplus \mathbf{1}$ tensors are marked in blue. Note that the last tensor class (in green) belongs to the $\mathcal{V} = \mathbf{6} \oplus \mathbf{6} \oplus \mathbf{10} \oplus \mathbf{\overline{10}} \oplus \mathbf{1}$ family of SU(4) symmetric tensors.

Occupation number	SU(4)	SU(6)
{0, 1, 0, 3}	4	0
{0, 1, 1, 2}	12	0
{0, 1, 2, 1}	36	0
{0, 1, 3, 0}	40	0
{0, 3, 0, 1}	12	0
{0, 3, 1, 0}	24	0
{1, 0, 0, 3}	4	4
{1, 0, 1, 2}	12	0
{1, 0, 2, 1}	36	24
{1, 0, 3, 0}	40	0
{1, 2, 0, 1}	36	0
{1, 2, 1, 0}	72	0
{2, 1, 0, 1}	36	24
{2, 1, 1, 0}	72	0
{3, 0, 0, 1}	12	0
{3, 0, 1, 0}	24	0
{0, 2, 1, 0}	0*	12

$D = 33$ virtual spaces,

$$\mathcal{V}_6 = \square \oplus \begin{array}{c}\square\\\square\\\square\end{array} \oplus \begin{array}{c}\square\\\square\end{array} \oplus \bullet \equiv \mathbf{6} \oplus \mathbf{\bar{6}} \oplus \mathbf{20} \oplus \mathbf{1}, \qquad (13)$$

for SU(6), and

$$\mathcal{V} = \begin{array}{c}\square\\\square\end{array} \oplus \square\square \oplus \square\square\square \oplus \bullet \equiv \mathbf{6} \oplus \mathbf{6}^* \oplus \mathbf{20}' \oplus \mathbf{1}, \qquad (14)$$

for SU(4), as listed in Table II. Only three occupation numbers fits SU(6) fusion rules, defining one more V class in addition to the two previous ones, as summarized in Table III. Since a large bond dimension $D = 33$ is untractable with current algorithms, in the following we shall use, in addition to the T tensors, the W tensors with $D = 13$.

TABLE III. SU(4)-symmetric tensors with $D \leqslant 33$ accommodating higher $\mathbf{6\bar{6}}$ SU(6) symmetry, classified according to their virtual space and occupation numbers in the $D = 33$ largest SU(4) virtual space.

Class	D	$\mathcal{V}$	n_{occ} [D=33]
T_0	7	$\mathbf{6} \oplus \mathbf{1}$	{1, 0, 0, 3}
W	13	$\mathbf{6} \oplus \mathbf{6} \oplus \mathbf{1}$	{2, 1, 0, 1}
V	33	$\mathbf{6} \oplus \mathbf{6} \oplus \mathbf{20} \oplus \mathbf{1}$	{1, 0, 2, 1}

V. TENSOR NETWORK ALGORITHMS

The energy density (i.e., the energy per site) or local observables of our SU(4)-symmetric PEPS can be computed efficiently using a corner transfer matrix renormalization group (CTMRG) algorithm (see, e.g., Ref. [23] for details). It is based on a real space RG scheme, adding a single site at a time (starting from a corner) to construct an effective environment around some active region—typically a small 2×1 or 2×2 cluster—involving corner C and edge T "fixed point" SU(4)-symmetric tensors. A parameter χ controls the amount of entanglement which is kept at each RG step in the Schmidt decomposition of the corner and, eventually, a $\chi \to \infty$ scaling is performed. Typically, a $1/D^2$ fraction of the new CTM eigenvalues are kept at each stage. The CTMRG enables then to compute the energy densities $\epsilon[\theta, \{a_i\}, \chi]$ of the various PEPS ansatz in Hamiltonian Eq. (2) (for each chosen θ value).

We then need to optimize the few coefficients $\{a_i\}$ of the tensors to minimize the above PEPS variational energies. After starting from an initial arbitrary choice of the tensor coefficients, using CTMRG we obtain the converged environment tensors C and T. We then evaluate the energy gradient numerically to "feed" a conjugate gradient (CG) algorithm minimization routine which provides a new set of parameters. The procedure is repeated until the energy minimum is found. To take into account the error induced by the finite corner dimension χ, we optimize the parameters for increasing χ, starting from the previously optimized set of parameters. When a maximal value of χ is reached (imposed by computer power limitations), we use finite-entanglement scaling to extrapolate the energy in the $\chi \to \infty$ limit.

The converged environment can then be used to compute the expectation value of any observable. It also allows to approximate the transfer matrix of an infinite one-dimensional (horizontal) strip obtained by contracting the TN in one (vertical) direction. From the two largest eigenvalues $\lambda_1 > \lambda_2$ of this transfer matrix, one can compute the largest correlation length $\xi = 1/\ln(\lambda_1/\lambda_2)$ of the system. From its leading eigenvector, one can also obtain the environment entanglement entropy S_{Env}, defined from a bipartition of the infinite strip (see Ref. [19] for the technical details).

VI. NUMERICAL RESULTS

A. Ground-state and variational energies

In Fig. 5(a), we have plotted, as a function of $\theta \in [-\pi, \pi]$, the energy density of some of the best low-energy PEPS, along with the finite-size ED energies and the exact ferromagnetic and four-site plaquette order wave functions (see Appendix A for details). As mentioned before, the ferromagnetic phase is exactly confined outside of the range $-3\pi/4 \leqslant \theta \leqslant \pi/2$. Although an exact expression for the energy of the quantum antiferromagnetic state is not known, the latter is believed to be stable in some extended region $\theta \in [\theta_{\mathrm{AF}}, \theta_X]$ around $\theta = 0$. The two regions on each side of this AF phase, $-3\pi/4 \leqslant \theta \leqslant \theta_{\mathrm{AF}}$ and $\theta_X \leqslant \theta \leqslant \pi/2$ are likely to be SU(4)-symmetric
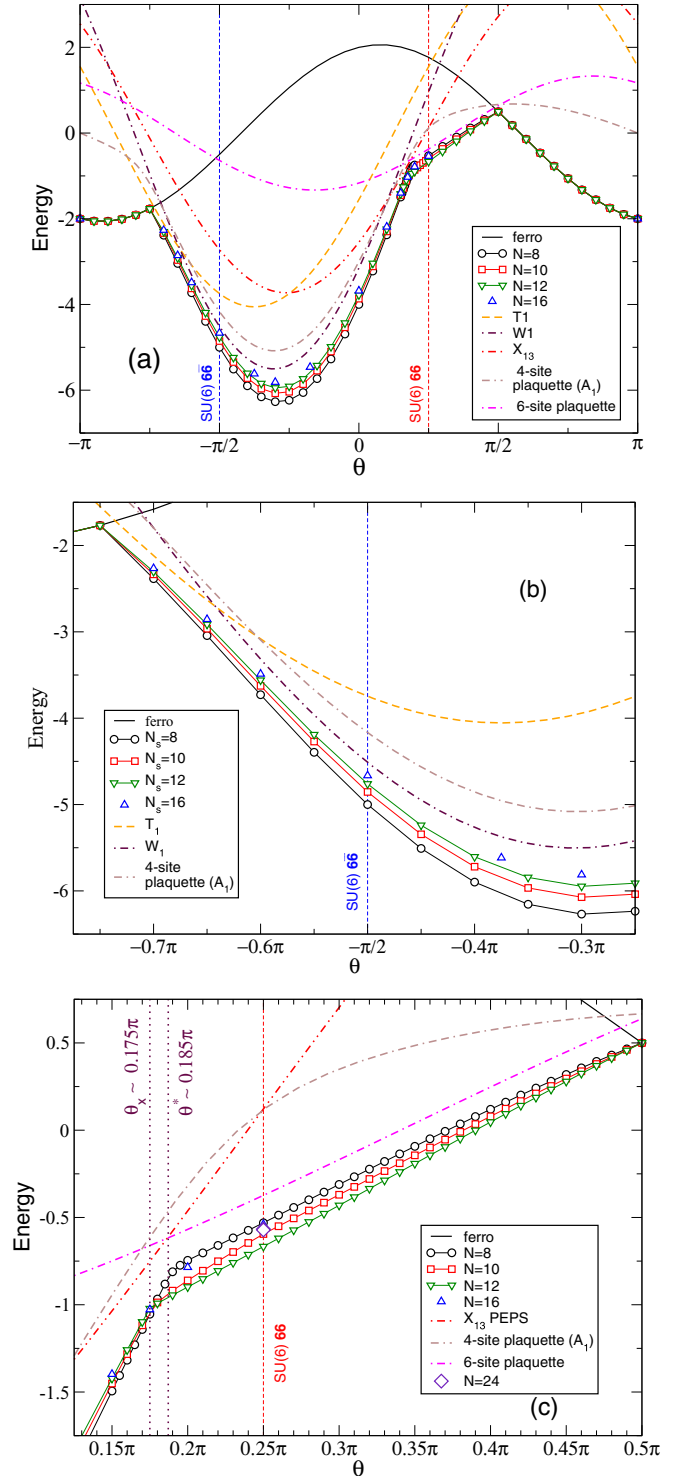
FIG. 5. Energies $\epsilon(\theta)$ of different wave functions under the Hamiltonian $\mathcal{H}(\theta)$. The PEPS energies are obtained after $\chi \to \infty$ extrapolation and compared to the exact ferromagnetic state $\mathcal{FM}$, to four-site and six-site plaquette VBCs (see text) and to ED of small clusters. The red points correspond to the optimization of the PEPS given by the $V = \mathbf{6} \oplus \mathbf{1}$ tensor (9). (a) Full parameter range $-\pi \leqslant \theta \leqslant \pi$. (b) Zoom of the range $-0.775\pi \leqslant \theta \leqslant 0.35\pi$. (c) Zoom of the range $0.125\pi \leqslant \theta \leqslant 0.5\pi$.

quantum disordered phases of different nature, breaking or not lattice symmetry, and we examine them separately.

B. Quantum disordered QD3 region

We first zoom in on the region $-3\pi/4 \leqslant \theta \lesssim \theta_{AF}$ in Fig. 5(b). In this region, Paramekanti and Marston proposed a phase transition from the ferromagnetic phase to a dimerized phase. According to their VMC calculation the dimerorder parameter of the best optimized (projected) dimerized state is close to fully saturated close to the transition with the ferromagnetic state. In other words, according to them, coupling dimers (within their variational manifold) does not decrease the energy. Although Paramekanti *et al.* do not quote any energy, we could nevertheless (approximately) estimate their best variational energy using a decoupled dimer meanfield solution (see Appendix A) and we found the energy of our uniform PEPS is significantly lower. This does not exclude that a small dimerization could take place but this definitely shows that our ansatz is better than Paramekanti's (projected) dimerized state when approaching the transition to the ferromagnet at $\theta = -3\pi/4$. Here the optimum PEPS is obtained for $a_1 \gg a_0, a_2, a_3$ (within the accuracy of our minimization for $\chi = D^2$)—i.e., it is basically given by the T_1 tensor alone—so it does not break time-reversal symmetry and may be critical (or have a very long dimer correlation length). As shown in Figs. 6(a) and 6(b) the finite-χ extrapolation of the optimum PEPS energy, performed for $\theta = -0.7\pi$ and $\theta = -0.65\pi$, respectively, are in excellent agreement with finite-size scalings of ED and DMRG energies [24]. We therefore believe that this PEPS provides a good ground state candidate in this range of parameter and expect a QSL phase there.

Within this QD3 region, when moving towards the SU(6) $\mathbf{6\bar{6}}$ point, the variational energy of the A_T PEPS family deteriorates. However, as seen in Fig. 5(b), we have found that the variational energy of the staggered PEPS constructed by putting the W_1 ($\overline{W}_1$) $D = 13$ tensor on the A (B) sites becomes remarkably good within a wide region around the SU(6) point. This is clear from the comparison of the finite-χ extrapolation of the PEPS energy with finite-size ED and DMRG extrapolations, shown in Figs. 6(c) and 6(d) for $\theta = -0.5\pi$ and $\theta = -0.3\pi$, respectively. Early quantum Monte Carlo (QMC) accurate simulations at the SU(6) point (at which the minus-sign problem disappears) gave evidence for a dimerized phase, although with a quite small order parameter. In contrast, it is easy to see that our simple ansatz based on the [SU(6)-symmetric] W_1 tensor describes a nondegenerate translation invariant QSL. Nevertheless, due to a U(1) PEPS gauge symmetry, we expect its SU(6)-dimer correlations to be power-law so that this critical QSL can be viewed as a melted dimer-ordered state. Since the estimated correlation length of the dimer phase $\xi_{\mathbf{6\bar{6}}} \sim 5.4$ is relatively long and the PEPS energy is remarkably close to the QMC energy [see Fig. 6(c)], we believe the latter gives a faithful representation of the ground state at not too long distances compared to $\xi_{\mathbf{6\bar{6}}}$.

C. Quantum disordered QD1 and QD2 regions

We now consider the region $\theta_X \sim 0.175\pi \leqslant \theta \leqslant \theta^*$ where θ^* is close to the value $\theta^*_{1D} = \arctan(2/3) \simeq 0.187\pi$, corre-
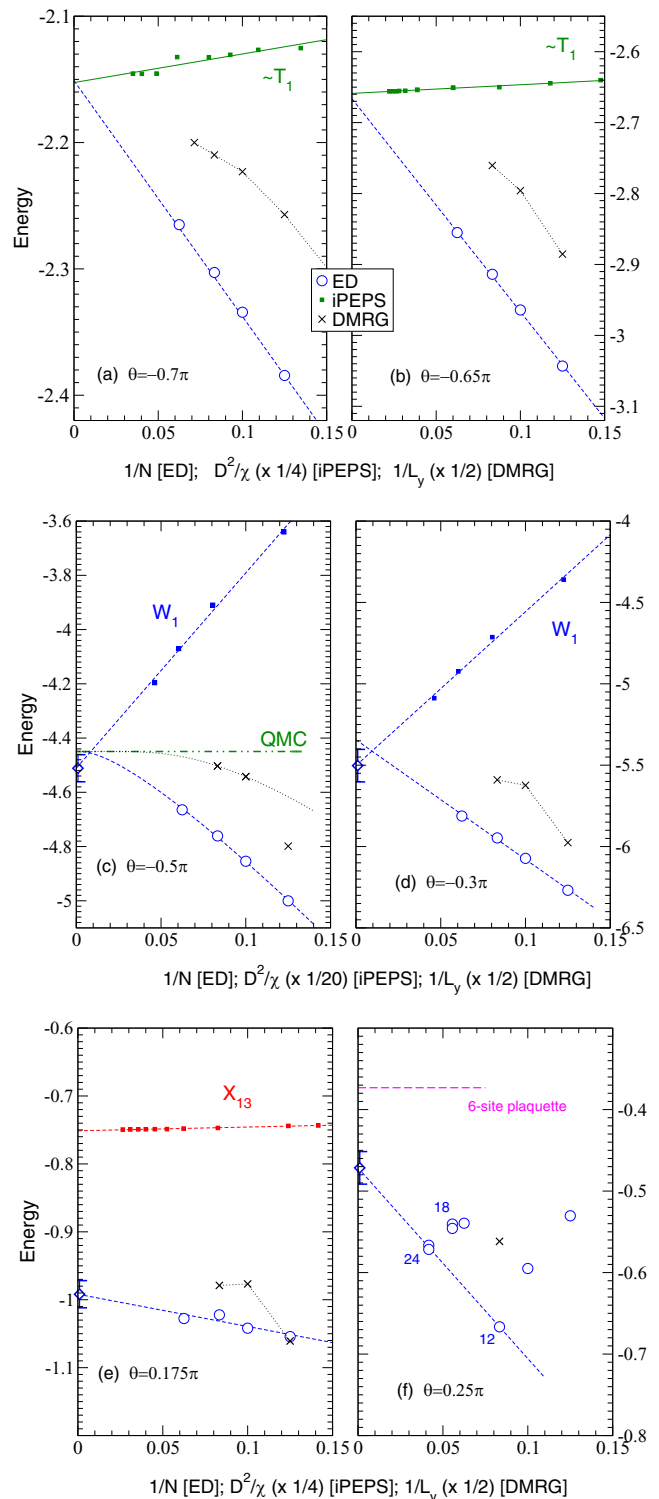
FIG. 6. Comparison of ED, DMRG, and iPEPS energy densities for various values of θ, as indicated on plots. Finite-size (finite χ) scaling is shown for ED periodic clusters and open DMRG cylinders (iPEPS infinite systems). Different PEPS are considered: T_1 (a), (b), W_1 (c), (d), and X_{13} (e). In panel (c), finite-size scalings of the ED and DMRG data are attempted as $\epsilon = e_{QMC} - ax \exp{-b/x}$, where $x = 1/\sqrt{N}$ and $x = 1/L_y$, respectively, and e_{QMC} is the (exact) QMC energy, providing estimates $\xi_{\mathbf{6\bar{6}}} = 1/b$ of the correlation length ~ 4.4 and ~ 5.4. Otherwise, crude linear fits in x are shown. The variational energy of the SU(6) six-site plaquette phase is reported in panel (f).

sponding to an exact point in 1D. There, Paramekanti and Marston propose two possibilities, either a direct transition from a Néel phase to a charge-conjugation breaking phase or a thin QSL phase. ED curves show a stark slope change around $\theta_X = 0.175\pi$, where we locate the transition from the AF state.

In our case, the tensors obtained from the X and Y family give a good energy in this region, a zoom on it is shown in Fig. 5(c). Initial results obtained with the full form of Eq. (11) show that charge conjugation is maximally broken in this region, therefore we thereafter restrict ourselves to $\alpha = \beta_{13}^{(i)} = 0$. In the 1D case, a MPS obtained from a similar construction gives the exact ground state for $\theta = \theta_{1D}^* = \arctan(2/3) \simeq 0.187\pi$. The estimation of the energy of the X_{31} PEPS [represented in Fig. 3(d)] is in reasonably good agreement with ED data as shown in Fig. 6(e). Note that this PEPS build from a single-site tensor bears some U(1) gauge symmetry so that we expect critical correlations. Indeed, Fig. 7(a) shows that the largest correlation length (obtained from the transfer operator) increases linearly with χ, with no sign of saturation. The scaling of the entanglement entropy S_{Env} w.r.t. the latter correlation length ξ according to the formula $S_{\text{Env}} = S_0 + c/6 \log \xi$ [25] in 7(a) suggests conformal field theory (CFT) criticality with central charge $c = 1$. Spin-spin and dimer-dimer correlations show very different qualitative behaviors, with exponential and algebraic decays, as shown in Figs. 7(c) and 7(d), respectively. While we expect the other PEPS [represented in Fig. 3(e)] obtained from the tensors Y_{202} and Y_{022} to be also relevant in this region (it is the simplest adaptation of the C-breaking phase construction of reference [15]), we were not able to compute an environment for these tensors. In any case, we expect a C-breaking phase that also breaks translation symmetry but preserves SU(4), as mimicked by our simplistic X_{31} PEPS. Slightly lower energies reached with nonzero $\beta_{31}^{(i)}$ indicate this phase may also break time-reversal symmetry.

For $\theta^* \leqslant \theta \leqslant \pi/2$, our best results were obtained with uncorrelated, singlet plaquettes of six sites (see Appendix A), which have better energies than our different PEPS ansatz as shown in Fig. 5(c). Such a plaquette can also be realized with the fundamental irrep of SU(6) on every site and indeed no special behavior is observed at the SU(6) point $\theta = \pi/4$. There is, however, a clear crossing of the energy curves at $\theta = \pi/2$, which corresponds to the transition to the FM state as discussed before. Hence, in this region, no evidence for a QSL phase is found, as the energies of our symmetry-preserving PEPS ansatz are well above.

VII. CONCLUSION

In this study, we have investigated the most general two-fermion SU(4)-symmetric Hamiltonian on the square lattice, with interaction limited to nearest-neighbor distance. We combined ED, DMRG, and PEPS techniques to propose a new phase diagram. We first argue the ferromagnetic domain is limited by the two SU(6) points at $\theta = \pi/2$ and $\theta = -3\pi/4$. We then explore the rest of the phase diagram using different PEPS ansatz and comparing them with DMRG and ED. We construct several SU(4) and C_{4v} symmetric PEPS, depending on very few parameters, and explain how to construct tensor
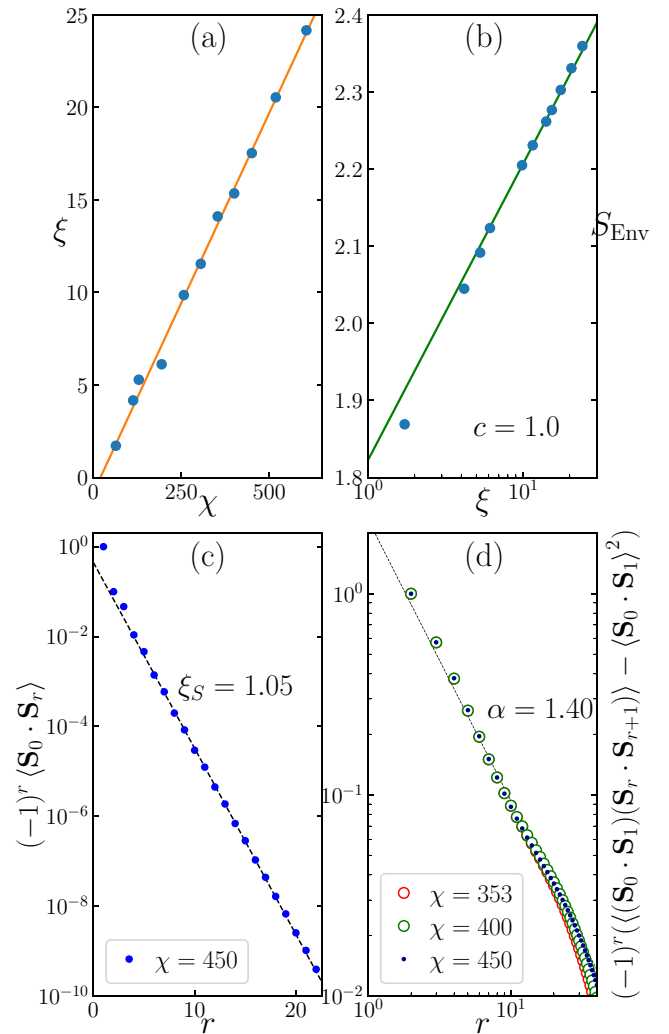
FIG. 7. Critical behavior of the X_{13}/X_{31} PEPS ansatz. (a) Largest correlation length ξ vs χ. (b) Scaling of the entanglement entropy vs. the log of ξ. A central charge $c = 1$ is proposed [25]. (c) Two-point (spin-spin) correlation function. An effective spin-spin correlation length is proposed with a fit $C_S(r + 1) = C_S(1) \exp(-r/\xi_S)$. (d) Four-point (dimer-dimer) correlation function, with critical exponent α fitted with $C_d(r + 1) = C_d(2) r^{-\alpha}$.

families that can capture the extended symmetry at the SU(6) points.

Previous QMC results on the SU(6) point $\theta = -\pi/2$ indicate a (weakly) dimerized phase there, and the purely bilinear point $\theta = 0$ is known to belong to the AF phase. Although the restriction to uniform symmetric PEPS prevents us from accessing dimerized and Néel phases, our PEPS still provide excellent variational energies in both (i) an extended region from the ferromagnetic boundary at $\theta = -3\pi/4$ all the way to $\theta \sim -0.30\pi$ (including the SU(6) dimerized point) and (ii) a narrower region around $\theta = 0.18\pi$. In the first region, due to the simplistic nature of the two low-energy best PEPS—they are build from a (fixed) single tensor encoding a continuous U(1) gauge symmetry—critical dimer correlations are found, which may be quite unstable [26,27]. Hence, minimal refinement of these PEPS wave functions could lead

to either (i) a short-ranged QSL with topological order—by breaking the continuous gauge symmetry to a discrete gauge symmetry—or (ii) a weakly dimerized phase—by allowing a two-sublattice modulation of the site tensor. Although, the second scenario agrees with the known physical behavior at the SU(6) point $\theta = -\pi/2$, the first scenario of a topological QSL may well be realized closer to the ferromagnetic phase transition at $\theta = -3\pi/4$.

In the narrower region around $\theta \sim 0.18\pi$, we found no evidence for a *uniform* QSL but, rather, a $q = (\pi, \pi)$-modulated charge conjugation-breaking phase. Such a phase is a natural generalization of the 1D C-breaking phase, and has a particularly simple PEPS representation. Our analysis also suggests a transition from this phase to a six-site plaquette phase, which seems to extend all the way to the ferromagnetic phase transition point at $\theta = \pi/2$. Of course, one cannot exclude that $\theta^* - \theta_x \to 0$, for increasing cluster sizes in ED, in which case one would observe a direct transition from the Néel state to the plaquette phase and no intermediate C-breaking phase.

Last, we note that SU(4) qualitatively differs from SU(2) where no QSL arises in the case of NN interactions only. This leaves open the possibility of experimental realizations using any ultracold alkaline-earth atoms realizing SU(N) symmetry by simply tuning the number of species [28] to, e.g., $N = 4$. Fixing a filling of two particles per site should avoid three-body losses and thus allow controlled experiments.

APPENDIX A: SIMPLE ANSATZ

We consider here a few simple exact SU(4) states on the square lattice to compare to our PEPS. These states correspond to magnetic or quantum disordered phases, some of them introduced in Ref. [16]. On a given lattice with coordination number z and nearest-neighbor coupling, the energy per site is one half of the average value of all the $\mathcal{H}(\theta)$ taken on the z bonds. The energy of a given wave function for all θ is a sinusoid parameterized by its value in two points only: $\langle \mathcal{H}(\theta) \rangle = \cos(\theta) \mathcal{H}(0) + \sin(\theta) \mathcal{H}(\pi/2)$.

1. Ferromagnetic state $\mathcal{FM}$

This state is the most symmetric and any pair of sites in the lattice is projected in the most symmetric irrep **20**. In this state, $\langle \mathcal{H}(\theta) \rangle_{\mathbf{20}} = \cos(\theta) + \frac{\sin \theta}{4}$ and, therefore, the energy per

site is

$$e_{\mathcal{FM}} = 2\cos\theta + \tfrac{1}{2}\sin\theta \qquad (A1)$$

2. Uncorrelated state $\mathcal{U}$

In this state, each site is totally uncorrelated from its neighbors, which means $\langle \mathcal{H}(\theta) \rangle_{\text{unc}} = \text{Tr}(\mathcal{H})/36 = \frac{5}{12}\sin\theta$. Hence, the energy per site is

$$e_{\mathcal{U}} = \tfrac{5}{6}\sin\theta. \qquad (A2)$$

3. Dimerized state $\mathcal{D}$

In a fully dimerized state, each site belongs to one singlet of energy $\langle \mathcal{H}(\theta) \rangle_{\mathbf{1}} = -5\cos(\theta) + \frac{25}{4}\sin\theta$. All the other neighbors are totally uncorrelated. Every dimer covering states have the same energy per site,

$$e_{\mathcal{D}} = -\tfrac{5}{2}\cos\theta + \tfrac{15}{4}\sin\theta. \qquad (A3)$$

4. Four-site plaquette states $\mathcal{P}_4$

On the square lattice we can also construct states where four sites in a square form a singlet and cover the lattice with these plaquettes. This state spontaneously breaks the translation invariance of the lattice. To construct it, we have to consider the projector $\square^{\otimes 4} \to \bullet$. Three independent singlets can be made on the square, they can easily be obtained by diagonalizing the quadratic Casimir operator on four sites. The point group C_{4v} naturally acts on this space and we can decompose the states in term of its irreducible representations: two singlets have $\mathcal{A}_1$ symmetry and the last one has $\mathcal{B}_2$ symmetry.

Diagonalizing $\mathcal{H}(\theta)$ on a four-site plaquette in this restricted subspace leads to three eigenvalues $8\sin(\theta) - 6\cos(\theta) \pm \sqrt{-76\sin(2\theta) - 13\cos(2\theta) + 85}/\sqrt{2}$ and $11\sin(\theta) - 8\cos(\theta)$. Covering the lattice with such plaquettes and taking into account that uncorrelated bonds contribute to the total energy per site according to Eq. (A2) we obtain the variational energies:

$$e_{\mathcal{P}_4}^{\mathcal{A}_1} = -\frac{3}{2}\cos\theta + \frac{29}{12}\sin\theta$$
$$\pm \frac{\sqrt{2}}{8}\sqrt{85 - 13\cos(2\theta) - 76\sin(2\theta)}, \quad (A4)$$

$$e_{\mathcal{P}_4}^{\mathcal{B}_2} = -2\cos\theta + \frac{19}{6}\sin\theta. \qquad (A5)$$

5. Six-site plaquette state $\mathcal{P}_6$

For a single six-site plaquette (3×2 rectangle), only one SU(6) singlet can be obtained if each site hosts the fundamental representation of SU(6). By construction, this state is antisymmetric with respect to any two-site permutation. In the SU(4) language [obtained by a simple identification of the six states of the fundamental representation of SU(6) and the six states of the **6** representation of SU(4)], this state can be viewed as a pairing of any pair of sites into the (antisymmetric) **15** representation of SU(4). As a consequence, it becomes obvious that this is an eigenstate of $\mathcal{H}(\theta)$ with the energy $7[-\cos\theta + (1/4)\sin\theta]$. As in the four-site plaquette

TABLE IV. List of clusters studied with ED: number of sites N_s, the two unit vectors, compatibility with a dimerized phase, and point-group symmetry.

Cluster	$\mathbf{t}_1$	$\mathbf{t}_2$	Can host a columnar phase	Point group
8	(2,2)	(−2, 2)	Yes	C_{4v}
10	(1,3)	(3, −1)	No	C_4
12	(1,3)	(4,0)	No	C_2
16	(4,0)	(0,4)	Yes	C_{4v}

states, the variational energy of the uniform covering of the lattice with such six-site plaquettes is given by

$$e_{\mathcal{P}_6} = -\tfrac{7}{6}\cos\theta + \tfrac{23}{36}\sin\theta. \tag{A6}$$

We only plot the ferromagnetic state, the lowest four-site plaquette state and the six-site plaquette state energies as a function of θ.

APPENDIX B: ADDITIONAL INFORMATION FOR EXACT DIAGONALIZATION

For exact diagonalization, we have computed the ground-state and low-energy excitations using a Lanczos algorithm on several finite-size clusters of N_s sites with periodic boundary conditions, see Table IV. Since we are mostly looking for a quantum spin liquid state, we have considered clusters that can accommodate the columnar phase [i.e., possess $(\pi, 0)$ and $(0, \pi)$ momenta in their Brillouin zone] or not. Moreover, we have also considered one cluster ($N_s = 12$) which is not a perfect square since its unit vectors are not perpendicular, which is not an issue for disordered phase [30]. Last, to reduce the size of the Hilbert space, we have used all space symmetries (translation and point-group) as well as the 3 Cartan U(1) symmetries (color conservation).

APPENDIX C: PEPS WITH HIGHER $\mathbf{6\bar{6}}$ SU(6) SYMMETRY

We now focus on the SU(6) $\mathbf{6\bar{6}}$ symmetric point at $\theta = \pi/4$ [for which the GS is a nondegenerate SU(6) singlet on finite clusters] and extend the tensor construction in such a way that

TABLE V. Eleven classes of SU(4)-symmetric tensors which can accomodate SU(6)-symmetry, classified according to their virtual space and occupation numbers in the $D = 43$ largest SU(4) virtual space.

Class	D	$\mathcal{V}$	$n_{\mathrm{occ}\,[D=43]}$
T_0	7	$\mathbf{6}\oplus\mathbf{1}$	{1, 0, 0, 0, 3}
W	13	$\mathbf{6}\oplus\mathbf{6}\oplus\mathbf{1}$	{2, 1, 0, 0, 1}
R_1	43	$\mathbf{6}\oplus\mathbf{6}\oplus\mathbf{15}\oplus\mathbf{15}\oplus\mathbf{1}$	{3, 0, 0, 1, 0}
R_2	43	$\mathbf{6}\oplus\mathbf{6}\oplus\mathbf{15}\oplus\mathbf{15}\oplus\mathbf{1}$	{1, 2, 1, 0, 0}
R_3	43	$\mathbf{6}\oplus\mathbf{6}\oplus\mathbf{15}\oplus\mathbf{15}\oplus\mathbf{1}$	{1, 0, 3, 0, 0}
R_4	43	$\mathbf{6}\oplus\mathbf{6}\oplus\mathbf{15}\oplus\mathbf{15}\oplus\mathbf{1}$	{1, 0, 1, 1, 1}
R_5	43	$\mathbf{6}\oplus\mathbf{6}\oplus\mathbf{15}\oplus\mathbf{15}\oplus\mathbf{1}$	{1, 0, 0, 3, 0}
R_6	43	$\mathbf{6}\oplus\mathbf{6}\oplus\mathbf{15}\oplus\mathbf{15}\oplus\mathbf{1}$	{0, 3, 0, 1, 0}
R_7	43	$\mathbf{6}\oplus\mathbf{6}\oplus\mathbf{15}\oplus\mathbf{15}\oplus\mathbf{1}$	{0, 1, 2, 1, 0}
R_8	43	$\mathbf{6}\oplus\mathbf{6}\oplus\mathbf{15}\oplus\mathbf{15}\oplus\mathbf{1}$	{0, 1, 1, 0, 2}
R_9	43	$\mathbf{6}\oplus\mathbf{6}\oplus\mathbf{15}\oplus\mathbf{15}\oplus\mathbf{1}$	{0, 1, 0, 2, 1}
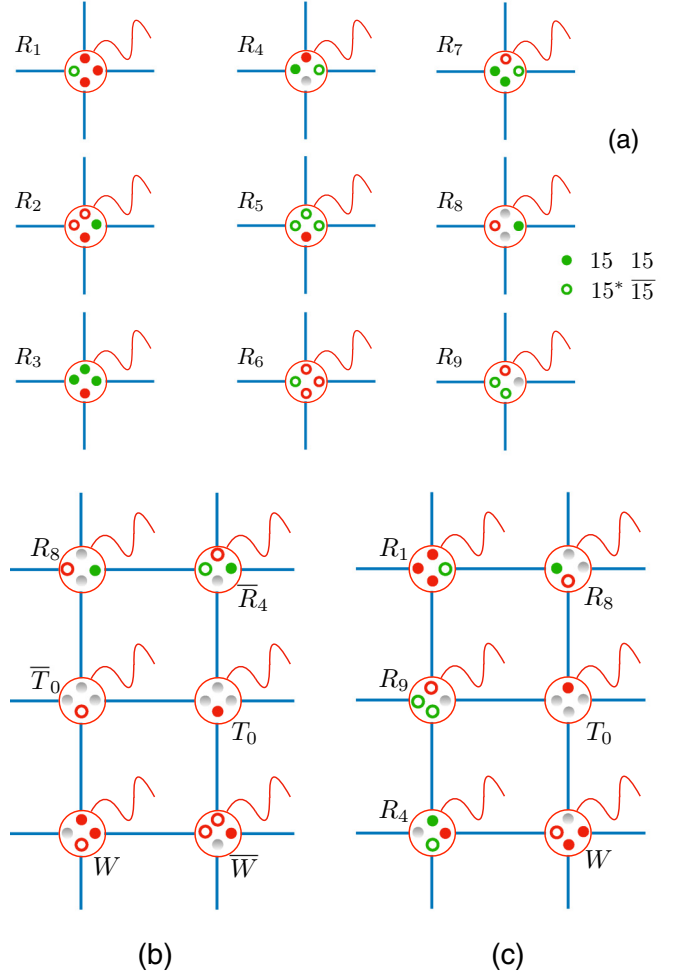
FIG. 8. (a) The nine R_i classes of $D = 43$ tensors that can acco-modate SU(6) fusion rules—see Table V. Color-conjugated tensors (same tensors) have to be used on the A and B sites to accomodate the $\mathbf{6\bar{6}}$ ($\mathbf{\bar{6}6}$) SU(6) symmetry as shown in panels (b) and (c), respectively.

the PEPS now inherits the enlarged symmetry. If we try to start from the previous SU(6) virtual space $\mathcal{V}_6 = \mathbf{6}\oplus\mathbf{\bar{6}}\oplus\mathbf{1}$, then we are now left with tensors whose occupation numbers should be restricted to $n_{\mathrm{occ}} = \{1, 0, 3\}$ or $n_{\mathrm{occ}} = \{2, 1, 1\}$ on *both* A and B sites. It is easy to check that it is *impossible* to pave the square lattice with such tensors assuming the pairs of virtual states on the bonds are contracted into ●● or $\mathbf{6\bar{6}}$ singlets. The same conclusion holds for $\mathcal{V}_6 = \mathbf{6}\oplus\mathbf{\bar{6}}\oplus\mathbf{20}\oplus\mathbf{1}$. We are there forced to introduce new/extra virtual degrees of freedom. The simplest choice of the SU(6) virtual space is

$$\mathcal{V}_6 = \square \oplus \begin{smallmatrix}\square\\\square\\\square\\\square\end{smallmatrix} \oplus \square\square \oplus \begin{smallmatrix}\square\square\\\square\square\end{smallmatrix} \oplus \bullet \equiv \mathbf{6}\oplus\mathbf{\bar{6}}\oplus\mathbf{15}\oplus\overline{\mathbf{15}}\oplus\mathbf{1}, \tag{C1}$$

of dimension $D = 43$. The corresponding PEPS tensors represent all the fusion channels of four of the five species of Eq. (C1) onto the physical state $\mathbf{6}$. Mapping to SU(4) would

TABLE VI. Full list of the classes of $D = 43$ ($\mathbf{6} \oplus \mathbf{6} \oplus \mathbf{15} \oplus \mathbf{15} \oplus \mathbf{1}$) SU(4) symmetric tensors in terms of the occupation numbers of the five virtual particles. The second (third) column shows the number of SU(4) (SU(6)) fusion channels—i.e., the total number of SU(N) symmetric tensors (that could be further classified in terms of the irreps of the C_{4v} point group, $\mathcal{A}_1$, $\mathcal{A}_2$, $\mathcal{B}_1$, $\mathcal{B}_2$ and $\mathcal{E}$). The $\mathbf{6} \oplus \mathbf{1}$ T_0 tensor is marked in red. The $\mathbf{6} \oplus \mathbf{6} \oplus \mathbf{1}$ tensors are marked in blue. Note that the total occupancy of the $\mathbf{6}$ particles is odd, reflecting a gauge $\mathbb{Z}_2$ symmetry.

Occupation number	SU(4)	SU(6)
{0, 1, 0, 0, 3}	4	0
{0, 1, 0, 1, 2}	12	0
{0, 1, 0, 2, 1}	48	12
{0, 1, 0, 3, 0}	64	0
{0, 1, 1, 0, 2}	12	12
{0, 1, 1, 1, 1}	96	0
{0, 1, 1, 2, 0}	192	0
{0, 1, 2, 0, 1}	48	0
{0, 1, 2, 1, 0}	192	48
{0, 1, 3, 0, 0}	64	0
{0, 3, 0, 0, 1}	12	0
{0, 3, 0, 1, 0}	28	4
{0, 3, 1, 0, 0}	28	0
{1, 0, 0, 0, 3}	4	4
{1, 0, 0, 1, 2}	12	0
{1, 0, 0, 2, 1}	48	0
{1, 0, 0, 3, 0}	64	12
{1, 0, 1, 0, 2}	12	0
{1, 0, 1, 1, 1}	96	48
{1, 0, 1, 2, 0}	192	0
{1, 0, 2, 0, 1}	48	0
{1, 0, 2, 1, 0}	192	0
{1, 0, 3, 0, 0}	64	12
{1, 2, 0, 0, 1}	36	0
{1, 2, 0, 1, 0}	84	0
{1, 2, 1, 0, 0}	84	36
{2, 1, 0, 0, 1}	36	24
{2, 1, 0, 1, 0}	84	0
{2, 1, 1, 0, 0}	84	0
{3, 0, 0, 0, 1}	12	0
{3, 0, 0, 1, 0}	28	12
{3, 0, 1, 0, 0}	28	0

require a virtual space with irreps of the same dimensions,

$$\mathcal{V} = \square \oplus \square \oplus \begin{array}{c}\square\square\\\square\end{array} \oplus \begin{array}{c}\square\square\\\square\end{array} \oplus \bullet \qquad \text{(C2)}$$

$$\equiv \mathbf{6} \oplus \mathbf{6}^* \oplus \mathbf{15} \oplus \mathbf{15}^* \oplus \mathbf{1} ,$$

where both the $\mathbf{6}$ (self-conjugate) and $\mathbf{15}$ (adjoint) irreps occurs with multiplicity 2, i.e., with two "colors." Again, we use an * to distinguish the two copies. Unfortunately such a large $D = 43$ bond dimension is untractable.

To accomodate SU(6) fusion channels, we are left with only eleven classes defined by their possible occupations n_{occ} of the five virtual particles, as shown in Table V. The corresponding (classes of) tensors are drawn in Fig. 8(a).

TABLE VII. Gauge symmetries of the various SU(4)-symmetric tensor families and of their imbeded SU(6)-symmetric subfamilies, if they exist. The last two columns indicate whether (✓) or not (×) the SU(6) symmetric tensors can describe the $\mathbf{6}\bar{\mathbf{6}}$ and $\mathbf{66}$ symmetric points, respectively.

D	$\mathcal{V}$	$SU(4)/SU(6)$	$\mathbf{6\bar{6}}$	$\mathbf{66}$
7	$\mathbf{6} \oplus \mathbf{1}$	$\mathbb{Z}_2/\mathbb{Z}_2$	✓	×
8	$\mathbf{4} \oplus \bar{\mathbf{4}}$	$\mathbb{Z}_2/-$	–	–
9	$\mathbf{4} \oplus \bar{\mathbf{4}} \oplus \mathbf{1}$	$\mathbb{Z}_4/-$	–	–
13	$\mathbf{6} \oplus \mathbf{6} \oplus \mathbf{1}$	$\mathbb{Z}_2/\mathbb{Z}_6$	✓	×
15	$\mathbf{4} \oplus \bar{\mathbf{4}} \oplus \mathbf{6} \oplus \mathbf{1}$	$\mathbb{Z}_4/-$	–	–
21	$\mathbf{4} \oplus \bar{\mathbf{4}} \oplus \mathbf{6} \oplus \mathbf{6} \oplus \mathbf{1}$	$\mathbb{Z}_4/-$	–	–
33	$\mathbf{6} \oplus \mathbf{6} \oplus \mathbf{20} \oplus \mathbf{1}$	$\mathbb{Z}_2/\mathbb{Z}_6$	✓	×
43	$\mathbf{6} \oplus \mathbf{6} \oplus \mathbf{15} \oplus \mathbf{15} \oplus \mathbf{1}$	$\mathbb{Z}_2/\mathbb{Z}_6$	✓	✓
63	$\mathbf{6} \oplus \mathbf{6} \oplus \mathbf{15} \oplus \mathbf{15} \oplus \mathbf{20} \oplus \mathbf{1}$	$\mathbb{Z}_2/\mathbb{Z}_6$	✓	✓

Possible configurations of the PEPS after contracting some of these tensors is shown on Figs. 8(b) and 8(c). The full tensor classification of the $D = 43$ virtual space is given in Table VI.

Note that the C-symmetry corresponding to charge conjugation in the SU(6) case (and acts on the physical space as well) maps, in the SU(4) case, to a *gauge* symmetry $\mathcal{C}$ defined as color exchange acting only on the virtual space. Since the C symmetry is explicitly broken in the SU(6) PEPS (by construction, enforcing the physical irrep $\mathbf{6}$ on every site), its related gauge symmetry has to be broken in a very specific way in the corresponding SU(4) PEPS, as, e.g., shown in Table V. In fact, the gauge $\mathcal{C}$-symmetry can be decomposed as $\mathcal{C} = \mathcal{C}_1 \mathcal{C}_2$, where $\mathcal{C}_1$ and $\mathcal{C}_2$ color-exchange only the two $\mathbf{6}$ irreps or the two $\mathbf{15}$ irreps, respectively. These gauge transformations belong, in fact, to a larger SU(2) × SU(2) gauge group. Hence, three other classes of tensors can be easily obtained from the R_i classes by applying $\mathcal{C}_1$ only, $\mathcal{C}_2$ only or their product $\mathcal{C}$, respectively (see Table V). At the SU(6)-symmetric points, any one—but only one—of the four classes can be used to construct a SU(6) singlet. Note that for $\mathbf{6\bar{6}}$ SU(6) symmetry, the previous $\mathbf{6} \oplus \mathbf{6} \oplus \mathbf{1}$ PEPS can be extended using the eleven classes of $D = 43$ tensors on the A sites and their color-conjugate both in $\mathbf{6}$ and $\mathbf{15}$ of the B sites, as shown in Fig. 8(c).

APPENDIX D: GAUGE SYMMETRIES

The gauge symmetries of each of the tensor families can be viewed as charge conservation in the fusion process of the four virtual particles into the physical one. Therefore, one has to assign an integer charge to both virtual and physical degrees of freedom. It is natural to expect $\mathbb{Z}_4$ gauge symmetry for SU(4)-symmetric tensors in which case one should consider a minimal virtual space $\mathcal{V} = \mathbf{4} \oplus \bar{\mathbf{4}} \oplus \mathbf{6} \oplus \mathbf{1}$ to encode all particle types with charges $q = \{1, -1, 2, 0\}$ (mod 4) and the on-site charge conservation reads $q \cdot n_{\text{occ}} = 2$ (mod 4). However, it is easy to check that, for the virtual spaces that do not contain all four SU(4) charges, the gauge symmetry may be reduced to $\mathbb{Z}_2$, as shown in Table VII. For SU(6) symmetry, the $D = 63$ $\mathcal{V}_6 = \mathbf{6} \oplus \bar{\mathbf{6}} \oplus \mathbf{15} \oplus \overline{\mathbf{15}} \oplus \mathbf{20} \oplus \mathbf{1}$ tensors contains four of the six elementary virtual particles of charges $q_6 = \{1, -1, 2, -2, 3, 0\}$ (mod 6) and

TABLE VIII. Tensor X_{31} (multiplied by $4\sqrt{30}$).

$X_{31}[0, 0, 0, 3, 4] = 1$

$X_{31}[0, 0, 0, 4, 3] = 1$

$X_{31}[0, 0, 1, 5, 3] = 1$

$X_{31}[0, 0, 2, 6, 3] = 1$

$X_{31}[0, 0, 3, 0, 4] = -2$

$X_{31}[0, 0, 3, 1, 5] = -1$

$X_{31}[0, 0, 3, 2, 6] = -1$

$X_{31}[0, 0, 3, 3, 7] = -1$

$X_{31}[0, 0, 3, 4, 0] = 1$

$X_{31}[0, 0, 3, 5, 1] = 1$

$X_{31}[0, 0, 3, 6, 2] = 1$

$X_{31}[0, 0, 3, 7, 3] = 2$

$X_{31}[0, 0, 4, 0, 3] = -2$

$X_{31}[0, 0, 4, 3, 0] = 1$

$X_{31}[0, 0, 5, 1, 3] = -1$

$X_{31}[0, 0, 6, 2, 3] = -1$

$X_{31}[0, 0, 7, 3, 3] = -1$

$X_{31}[0, 1, 0, 3, 5] = 1$

$X_{31}[0, 1, 3, 0, 5] = -1$

$X_{31}[0, 1, 5, 0, 3] = -1$

$X_{31}[0, 1, 5, 3, 0] = 1$

$X_{31}[0, 2, 0, 3, 6] = 1$

$X_{31}[0, 2, 3, 0, 6] = -1$

$X_{31}[0, 2, 6, 0, 3] = -1$

$X_{31}[0, 2, 6, 3, 0] = 1$

$X_{31}[0, 3, 0, 0, 4] = 1$

$X_{31}[0, 3, 0, 1, 5] = 1$

$X_{31}[0, 3, 0, 2, 6] = 1$

$X_{31}[0, 3, 0, 3, 7] = 2$

$X_{31}[0, 3, 0, 4, 0] = -2$

$X_{31}[0, 3, 0, 5, 1] = -1$

$X_{31}[0, 3, 0, 6, 2] = -1$

$X_{31}[0, 3, 0, 7, 3] = -1$

$X_{31}[0, 3, 1, 5, 0] = -1$

$X_{31}[0, 3, 2, 6, 0] = -1$

$X_{31}[0, 3, 3, 0, 7] = -1$

$X_{31}[0, 3, 3, 7, 0] = -1$

$X_{31}[0, 3, 4, 0, 0] = 1$

$X_{31}[0, 3, 5, 1, 0] = 1$

$X_{31}[0, 3, 6, 2, 0] = 1$

$X_{31}[0, 3, 7, 0, 3] = -1$

$X_{31}[0, 3, 7, 3, 0] = 2$

$X_{31}[0, 4, 0, 0, 3] = 1$

$X_{31}[0, 4, 0, 3, 0] = -2$

$X_{31}[0, 4, 3, 0, 0] = 1$

$X_{31}[0, 5, 0, 3, 1] = -1$

$X_{31}[0, 5, 1, 0, 3] = 1$

$X_{31}[0, 5, 1, 3, 0] = -1$

$X_{31}[0, 5, 3, 0, 1] = 1$

$X_{31}[0, 6, 0, 3, 2] = -1$

$X_{31}[0, 6, 2, 0, 3] = 1$

$X_{31}[0, 6, 2, 3, 0] = -1$

$X_{31}[0, 6, 3, 0, 2] = 1$

$X_{31}[0, 7, 0, 3, 3] = -1$

$X_{31}[0, 7, 3, 0, 3] = 2$

$X_{31}[0, 7, 3, 3, 0] = -1$

$X_{31}[1, 0, 0, 2, 4] = 1$

$X_{31}[1, 0, 0, 4, 2] = 1$

$X_{31}[1, 0, 1, 5, 2] = 1$

$X_{31}[1, 0, 2, 0, 4] = -2$

$X_{31}[1, 0, 2, 1, 5] = -1$

$X_{31}[1, 0, 2, 2, 6] = -1$

$X_{31}[1, 0, 2, 3, 7] = -1$

$X_{31}[1, 0, 2, 4, 0] = 1$

$X_{31}[1, 0, 2, 5, 1] = 1$

$X_{31}[1, 0, 2, 6, 2] = 2$

$X_{31}[1, 0, 2, 7, 3] = 1$

$X_{31}[1, 0, 3, 7, 2] = 1$

$X_{31}[1, 0, 4, 0, 2] = -2$

$X_{31}[1, 0, 4, 2, 0] = 1$

$X_{31}[1, 0, 5, 1, 2] = -1$

$X_{31}[1, 0, 6, 2, 2] = -1$

$X_{31}[1, 0, 7, 3, 2] = -1$

$X_{31}[1, 1, 0, 2, 5] = 1$

$X_{31}[1, 1, 2, 0, 5] = -1$

$X_{31}[1, 1, 5, 0, 2] = -1$

$X_{31}[1, 1, 5, 2, 0] = 1$

$X_{31}[1, 2, 0, 0, 4] = 1$

$X_{31}[1, 2, 0, 1, 5] = 1$

$X_{31}[1, 2, 0, 2, 6] = 2$

$X_{31}[1, 2, 0, 3, 7] = 1$

$X_{31}[1, 2, 0, 4, 0] = -2$

$X_{31}[1, 2, 0, 5, 1] = -1$

$X_{31}[1, 2, 0, 6, 2] = -1$

$X_{31}[1, 2, 0, 7, 3] = -1$

$X_{31}[1, 2, 1, 5, 0] = -1$

$X_{31}[1, 2, 2, 0, 6] = -1$

$X_{31}[1, 2, 2, 6, 0] = -1$

$X_{31}[1, 2, 3, 7, 0] = -1$

$X_{31}[1, 2, 4, 0, 0] = 1$

$X_{31}[1, 2, 5, 1, 0] = 1$

$X_{31}[1, 2, 6, 0, 2] = -1$

$X_{31}[1, 2, 6, 2, 0] = 2$

$X_{31}[1, 2, 7, 3, 0] = 1$

$X_{31}[1, 3, 0, 2, 7] = 1$

$X_{31}[1, 3, 2, 0, 7] = -1$

$X_{31}[1, 3, 7, 0, 2] = -1$

$X_{31}[1, 3, 7, 2, 0] = 1$

$X_{31}[1, 4, 0, 0, 2] = 1$

$X_{31}[1, 4, 0, 2, 0] = -2$

$X_{31}[1, 4, 2, 0, 0] = 1$

$X_{31}[1, 5, 0, 2, 1] = -1$

$X_{31}[1, 5, 1, 0, 2] = 1$

$X_{31}[1, 5, 1, 2, 0] = -1$

$X_{31}[1, 5, 2, 0, 1] = 1$

$X_{31}[1, 6, 0, 2, 2] = -1$

$X_{31}[1, 6, 2, 0, 2] = 2$

$X_{31}[1, 6, 2, 2, 0] = -1$

$X_{31}[1, 7, 0, 2, 3] = -1$

$X_{31}[1, 7, 2, 0, 3] = 1$

$X_{31}[1, 7, 3, 0, 2] = 1$

$X_{31}[1, 7, 3, 2, 0] = -1$

$X_{31}[2, 0, 2, 3, 4] = 1$

$X_{31}[2, 0, 3, 2, 4] = -1$

$X_{31}[2, 0, 4, 2, 3] = -1$

$X_{31}[2, 0, 4, 3, 2] = 1$

$X_{31}[2, 1, 2, 3, 5] = 1$

$X_{31}[2, 1, 3, 2, 5] = -1$

$X_{31}[2, 1, 5, 2, 3] = -1$

$X_{31}[2, 1, 5, 3, 2] = 1$

$X_{31}[2, 2, 0, 4, 3] = 1$

$X_{31}[2, 2, 1, 5, 3] = 1$

$X_{31}[2, 2, 2, 3, 6] = 1$

$X_{31}[2, 2, 2, 6, 3] = 1$

$X_{31}[2, 2, 3, 0, 4] = -1$

$X_{31}[2, 2, 3, 1, 5] = -1$

$X_{31}[2, 2, 3, 2, 6] = -2$

$X_{31}[2, 2, 3, 3, 7] = -1$

$X_{31}[2, 2, 3, 4, 0] = 1$

$X_{31}[2, 2, 3, 5, 1] = 1$

$X_{31}[2, 2, 3, 6, 2] = 1$

$X_{31}[2, 2, 3, 7, 3] = 2$

$X_{31}[2, 2, 4, 0, 3] = -1$

$X_{31}[2, 2, 5, 1, 3] = -1$

$X_{31}[2, 2, 6, 2, 3] = -2$

$X_{31}[2, 2, 6, 3, 2] = 1$

$X_{31}[2, 2, 7, 3, 3] = -1$

$X_{31}[2, 3, 0, 4, 2] = -1$

$X_{31}[2, 3, 1, 5, 2] = -1$

$X_{31}[2, 3, 2, 0, 4] = 1$

$X_{31}[2, 3, 2, 1, 5] = 1$

$X_{31}[2, 3, 2, 2, 6] = 1$

$X_{31}[2, 3, 2, 3, 7] = 2$

$X_{31}[2, 3, 2, 4, 0] = -1$

$X_{31}[2, 3, 2, 5, 1] = -1$

$X_{31}[2, 3, 2, 6, 2] = -2$

$X_{31}[2, 3, 2, 7, 3] = -1$

$X_{31}[2, 3, 3, 2, 7] = -1$

$X_{31}[2, 3, 3, 7, 2] = -1$

$X_{31}[2, 3, 4, 0, 2] = 1$

$X_{31}[2, 3, 5, 1, 2] = 1$

$X_{31}[2, 3, 6, 2, 2] = 1$

$X_{31}[2, 3, 7, 2, 3] = -1$

$X_{31}[2, 3, 7, 3, 2] = 2$

$X_{31}[2, 4, 0, 2, 3] = 1$

$X_{31}[2, 4, 0, 3, 2] = -1$

$X_{31}[2, 4, 2, 3, 0] = -1$

$X_{31}[2, 4, 3, 2, 0] = 1$

$X_{31}[2, 5, 1, 2, 3] = 1$

$X_{31}[2, 5, 1, 3, 2] = -1$

$X_{31}[2, 5, 2, 3, 1] = -1$

$X_{31}[2, 5, 3, 2, 1] = 1$

$X_{31}[2, 6, 2, 2, 3] = 1$

$X_{31}[2, 6, 2, 3, 2] = -2$

$X_{31}[2, 6, 3, 2, 2] = 1$

$X_{31}[2, 7, 2, 3, 3] = -1$

$X_{31}[2, 7, 3, 2, 3] = 2$

$X_{31}[2, 7, 3, 3, 2] = -1$

$X_{31}[3, 0, 0, 1, 4] = 1$

$X_{31}[3, 0, 0, 4, 1] = 1$

$X_{31}[3, 0, 1, 0, 4] = -2$

$X_{31}[3, 0, 1, 1, 5] = -1$

$X_{31}[3, 0, 1, 2, 6] = -1$

$X_{31}[3, 0, 1, 3, 7] = -1$

$X_{31}[3, 0, 1, 4, 0] = 1$

$X_{31}[3, 0, 1, 5, 1] = 2$

$X_{31}[3, 0, 1, 6, 2] = 1$

$X_{31}[3, 0, 1, 7, 3] = 1$

$X_{31}[3, 0, 2, 6, 1] = 1$

$X_{31}[3, 0, 3, 7, 1] = 1$

TABLE VIII. (*Continued.*)

$X_{31}[3,0,4,0,1] = -2$	$X_{31}[3,0,4,1,0] = 1$	$X_{31}[3,0,5,1,1] = -1$
$X_{31}[3,0,6,2,1] = -1$	$X_{31}[3,0,7,3,1] = -1$	$X_{31}[3,1,0,0,4] = 1$
$X_{31}[3,1,0,1,5] = 2$	$X_{31}[3,1,0,2,6] = 1$	$X_{31}[3,1,0,3,7] = 1$
$X_{31}[3,1,0,4,0] = -2$	$X_{31}[3,1,0,5,1] = -1$	$X_{31}[3,1,0,6,2] = -1$
$X_{31}[3,1,0,7,3] = -1$	$X_{31}[3,1,1,0,5] = -1$	$X_{31}[3,1,1,5,0] = -1$
$X_{31}[3,1,2,6,0] = -1$	$X_{31}[3,1,3,7,0] = -1$	$X_{31}[3,1,4,0,0] = 1$
$X_{31}[3,1,5,0,1] = -1$	$X_{31}[3,1,5,1,0] = 2$	$X_{31}[3,1,6,2,0] = 1$
$X_{31}[3,1,7,3,0] = 1$	$X_{31}[3,2,0,1,6] = 1$	$X_{31}[3,2,1,0,6] = -1$
$X_{31}[3,2,6,0,1] = -1$	$X_{31}[3,2,6,1,0] = 1$	$X_{31}[3,3,0,1,7] = 1$
$X_{31}[3,3,1,0,7] = -1$	$X_{31}[3,3,7,0,1] = -1$	$X_{31}[3,3,7,1,0] = 1$
$X_{31}[3,4,0,0,1] = 1$	$X_{31}[3,4,0,1,0] = -2$	$X_{31}[3,4,1,0,0] = 1$
$X_{31}[3,5,0,1,1] = -1$	$X_{31}[3,5,1,0,1] = 2$	$X_{31}[3,5,1,1,0] = -1$
$X_{31}[3,6,0,1,2] = -1$	$X_{31}[3,6,1,0,2] = 1$	$X_{31}[3,6,2,0,1] = 1$
$X_{31}[3,6,2,1,0] = -1$	$X_{31}[3,7,0,1,3] = -1$	$X_{31}[3,7,1,0,3] = 1$
$X_{31}[3,7,3,0,1] = 1$	$X_{31}[3,7,3,1,0] = -1$	$X_{31}[4,0,1,3,4] = 1$
$X_{31}[4,0,3,1,4] = -1$	$X_{31}[4,0,4,1,3] = -1$	$X_{31}[4,0,4,3,1] = 1$
$X_{31}[4,1,0,4,3] = 1$	$X_{31}[4,1,1,3,5] = 1$	$X_{31}[4,1,1,5,3] = 1$
$X_{31}[4,1,2,6,3] = 1$	$X_{31}[4,1,3,0,4] = -1$	$X_{31}[4,1,3,1,5] = -2$
$X_{31}[4,1,3,2,6] = -1$	$X_{31}[4,1,3,3,7] = -1$	$X_{31}[4,1,3,4,0] = 1$
$X_{31}[4,1,3,5,1] = 1$	$X_{31}[4,1,3,6,2] = 1$	$X_{31}[4,1,3,7,3] = 2$
$X_{31}[4,1,4,0,3] = -1$	$X_{31}[4,1,5,1,3] = -2$	$X_{31}[4,1,5,3,1] = 1$
$X_{31}[4,1,6,2,3] = -1$	$X_{31}[4,1,7,3,3] = -1$	$X_{31}[4,2,1,3,6] = 1$
$X_{31}[4,2,3,1,6] = -1$	$X_{31}[4,2,6,1,3] = -1$	$X_{31}[4,2,6,3,1] = 1$
$X_{31}[4,3,0,4,1] = -1$	$X_{31}[4,3,1,0,4] = 1$	$X_{31}[4,3,1,1,5] = 1$
$X_{31}[4,3,1,2,6] = 1$	$X_{31}[4,3,1,3,7] = 2$	$X_{31}[4,3,1,4,0] = -1$
$X_{31}[4,3,1,5,1] = -2$	$X_{31}[4,3,1,6,2] = -1$	$X_{31}[4,3,1,7,3] = -1$
$X_{31}[4,3,2,6,1] = -1$	$X_{31}[4,3,3,1,7] = -1$	$X_{31}[4,3,3,7,1] = -1$
$X_{31}[4,3,4,0,1] = 1$	$X_{31}[4,3,5,1,1] = 1$	$X_{31}[4,3,6,2,1] = 1$
$X_{31}[4,3,7,1,3] = -1$	$X_{31}[4,3,7,3,1] = 2$	$X_{31}[4,4,0,1,3] = 1$
$X_{31}[4,4,0,3,1] = -1$	$X_{31}[4,4,1,3,0] = -1$	$X_{31}[4,4,3,1,0] = 1$
$X_{31}[4,5,1,1,3] = 1$	$X_{31}[4,5,1,3,1] = -2$	$X_{31}[4,5,3,1,1] = 1$
$X_{31}[4,6,1,3,2] = -1$	$X_{31}[4,6,2,1,3] = 1$	$X_{31}[4,6,2,3,1] = -1$
$X_{31}[4,6,3,1,2] = 1$	$X_{31}[4,7,1,3,3] = -1$	$X_{31}[4,7,3,1,3] = 2$
$X_{31}[4,7,3,3,1] = -1$	$X_{31}[5,0,1,2,4] = 1$	$X_{31}[5,0,2,1,4] = -1$
$X_{31}[5,0,4,1,2] = -1$	$X_{31}[5,0,4,2,1] = 1$	$X_{31}[5,1,0,4,2] = 1$
$X_{31}[5,1,1,2,5] = 1$	$X_{31}[5,1,1,5,2] = 1$	$X_{31}[5,1,2,0,4] = -1$
$X_{31}[5,1,2,1,5] = -2$	$X_{31}[5,1,2,2,6] = -1$	$X_{31}[5,1,2,3,7] = -1$
$X_{31}[5,1,2,4,0] = 1$	$X_{31}[5,1,2,5,1] = 1$	$X_{31}[5,1,2,6,2] = 2$
$X_{31}[5,1,2,7,3] = 1$	$X_{31}[5,1,3,7,2] = 1$	$X_{31}[5,1,4,0,2] = -1$
$X_{31}[5,1,5,1,2] = -2$	$X_{31}[5,1,5,2,1] = 1$	$X_{31}[5,1,6,2,2] = -1$
$X_{31}[5,1,7,3,2] = -1$	$X_{31}[5,2,0,4,1] = -1$	$X_{31}[5,2,1,0,4] = 1$
$X_{31}[5,2,1,1,5] = 1$	$X_{31}[5,2,1,2,6] = 2$	$X_{31}[5,2,1,3,7] = 1$
$X_{31}[5,2,1,4,0] = -1$	$X_{31}[5,2,1,5,1] = -2$	$X_{31}[5,2,1,6,2] = -1$
$X_{31}[5,2,1,7,3] = -1$	$X_{31}[5,2,2,1,6] = -1$	$X_{31}[5,2,2,6,1] = -1$
$X_{31}[5,2,3,7,1] = -1$	$X_{31}[5,2,4,0,1] = 1$	$X_{31}[5,2,5,1,1] = 1$
$X_{31}[5,2,6,1,2] = -1$	$X_{31}[5,2,6,2,1] = 2$	$X_{31}[5,2,7,3,1] = 1$
$X_{31}[5,3,1,2,7] = 1$	$X_{31}[5,3,2,1,7] = -1$	$X_{31}[5,3,7,1,2] = -1$
$X_{31}[5,3,7,2,1] = 1$	$X_{31}[5,4,0,1,2] = 1$	$X_{31}[5,4,0,2,1] = -1$
$X_{31}[5,4,1,2,0] = -1$	$X_{31}[5,4,2,1,0] = 1$	$X_{31}[5,5,1,1,2] = 1$
$X_{31}[5,5,1,2,1] = -2$	$X_{31}[5,5,2,1,1] = 1$	$X_{31}[5,6,1,2,2] = -1$
$X_{31}[5,6,2,1,2] = 2$	$X_{31}[5,6,2,2,1] = -1$	$X_{31}[5,7,1,2,3] = -1$
$X_{31}[5,7,2,1,3] = 1$	$X_{31}[5,7,3,1,2] = 1$	$X_{31}[5,7,3,2,1] = -1$

the SU(6) conservation rules state that $q_6 \cdot n_{\text{occ}} = 1 \pmod{6}$, providing the desired $\mathbb{Z}_6$ gauge symmetry. The gauge symmetry is also present for smaller bond dimension, except for $\mathcal{V}_6 = \mathbf{6} \oplus \mathbf{1}$, for which it is reduced to $\mathbb{Z}_2$, as shown in Table VII.

APPENDIX E: TENSOR EXPRESSIONS

The expression of the tensors T_i can be found in the Supplemental Material of Ref. [19]. We provide here the coefficients of the unnormalized tensors X_{31} (Table VIII) and W_1 (Table IX), which are integer values. The first index labels

TABLE IX. Tensor W_1 (multiplied by $12\sqrt{7}$).

$W_1[0, 0, 0, 6, 12] = 2$	$W_1[0, 0, 0, 12, 6] = 2$	$W_1[0, 0, 1, 7, 12] = 1$
$W_1[0, 0, 1, 12, 7] = 1$	$W_1[0, 0, 2, 8, 12] = 1$	$W_1[0, 0, 2, 12, 8] = 1$
$W_1[0, 0, 3, 9, 12] = 1$	$W_1[0, 0, 3, 12, 9] = 1$	$W_1[0, 0, 4, 10, 12] = 1$
$W_1[0, 0, 4, 12, 10] = 1$	$W_1[0, 0, 5, 11, 12] = 1$	$W_1[0, 0, 5, 12, 11] = 1$
$W_1[0, 0, 6, 0, 12] = 2$	$W_1[0, 0, 6, 12, 0] = 2$	$W_1[0, 0, 7, 1, 12] = 1$
$W_1[0, 0, 7, 12, 1] = 1$	$W_1[0, 0, 8, 2, 12] = 1$	$W_1[0, 0, 8, 12, 2] = 1$
$W_1[0, 0, 9, 3, 12] = 1$	$W_1[0, 0, 9, 12, 3] = 1$	$W_1[0, 0, 10, 4, 12] = 1$
$W_1[0, 0, 10, 12, 4] = 1$	$W_1[0, 0, 11, 5, 12] = 1$	$W_1[0, 0, 11, 12, 5] = 1$
$W_1[0, 0, 12, 0, 6] = 2$	$W_1[0, 0, 12, 1, 7] = 1$	$W_1[0, 0, 12, 2, 8] = 1$
$W_1[0, 0, 12, 3, 9] = 1$	$W_1[0, 0, 12, 4, 10] = 1$	$W_1[0, 0, 12, 5, 11] = 1$
$W_1[0, 0, 12, 6, 0] = 2$	$W_1[0, 0, 12, 7, 1] = 1$	$W_1[0, 0, 12, 8, 2] = 1$
$W_1[0, 0, 12, 9, 3] = 1$	$W_1[0, 0, 12, 10, 4] = 1$	$W_1[0, 0, 12, 11, 5] = 1$
$W_1[0, 1, 0, 7, 12] = 1$	$W_1[0, 1, 0, 12, 7] = 1$	$W_1[0, 1, 7, 0, 12] = 1$
$W_1[0, 1, 7, 12, 0] = 1$	$W_1[0, 1, 12, 0, 7] = 1$	$W_1[0, 1, 12, 7, 0] = 1$
$W_1[0, 2, 0, 8, 12] = 1$	$W_1[0, 2, 0, 12, 8] = 1$	$W_1[0, 2, 8, 0, 12] = 1$
$W_1[0, 2, 8, 12, 0] = 1$	$W_1[0, 2, 12, 0, 8] = 1$	$W_1[0, 2, 12, 8, 0] = 1$
$W_1[0, 3, 0, 9, 12] = 1$	$W_1[0, 3, 0, 12, 9] = 1$	$W_1[0, 3, 9, 0, 12] = 1$
$W_1[0, 3, 9, 12, 0] = 1$	$W_1[0, 3, 12, 0, 9] = 1$	$W_1[0, 3, 12, 9, 0] = 1$
$W_1[0, 4, 0, 10, 12] = 1$	$W_1[0, 4, 0, 12, 10] = 1$	$W_1[0, 4, 10, 0, 12] = 1$
$W_1[0, 4, 10, 12, 0] = 1$	$W_1[0, 4, 12, 0, 10] = 1$	$W_1[0, 4, 12, 10, 0] = 1$
$W_1[0, 5, 0, 11, 12] = 1$	$W_1[0, 5, 0, 12, 11] = 1$	$W_1[0, 5, 11, 0, 12] = 1$
$W_1[0, 5, 11, 12, 0] = 1$	$W_1[0, 5, 12, 0, 11] = 1$	$W_1[0, 5, 12, 11, 0] = 1$
$W_1[0, 6, 0, 0, 12] = 2$	$W_1[0, 6, 0, 12, 0] = 2$	$W_1[0, 6, 12, 0, 0] = 2$
$W_1[0, 7, 0, 1, 12] = 1$	$W_1[0, 7, 0, 12, 1] = 1$	$W_1[0, 7, 1, 0, 12] = 1$
$W_1[0, 7, 1, 12, 0] = 1$	$W_1[0, 7, 12, 0, 1] = 1$	$W_1[0, 7, 12, 1, 0] = 1$
$W_1[0, 8, 0, 2, 12] = 1$	$W_1[0, 8, 0, 12, 2] = 1$	$W_1[0, 8, 2, 0, 12] = 1$
$W_1[0, 8, 2, 12, 0] = 1$	$W_1[0, 8, 12, 0, 2] = 1$	$W_1[0, 8, 12, 2, 0] = 1$
$W_1[0, 9, 0, 3, 12] = 1$	$W_1[0, 9, 0, 12, 3] = 1$	$W_1[0, 9, 3, 0, 12] = 1$
$W_1[0, 9, 3, 12, 0] = 1$	$W_1[0, 9, 12, 0, 3] = 1$	$W_1[0, 9, 12, 3, 0] = 1$
$W_1[0, 10, 0, 4, 12] = 1$	$W_1[0, 10, 0, 12, 4] = 1$	$W_1[0, 10, 4, 0, 12] = 1$
$W_1[0, 10, 4, 12, 0] = 1$	$W_1[0, 10, 12, 0, 4] = 1$	$W_1[0, 10, 12, 4, 0] = 1$
$W_1[0, 11, 0, 5, 12] = 1$	$W_1[0, 11, 0, 12, 5] = 1$	$W_1[0, 11, 5, 0, 12] = 1$
$W_1[0, 11, 5, 12, 0] = 1$	$W_1[0, 11, 12, 0, 5] = 1$	$W_1[0, 11, 12, 5, 0] = 1$
$W_1[0, 12, 0, 0, 6] = 2$	$W_1[0, 12, 0, 1, 7] = 1$	$W_1[0, 12, 0, 2, 8] = 1$
$W_1[0, 12, 0, 3, 9] = 1$	$W_1[0, 12, 0, 4, 10] = 1$	$W_1[0, 12, 0, 5, 11] = 1$
$W_1[0, 12, 0, 6, 0] = 2$	$W_1[0, 12, 0, 7, 1] = 1$	$W_1[0, 12, 0, 8, 2] = 1$
$W_1[0, 12, 0, 9, 3] = 1$	$W_1[0, 12, 0, 10, 4] = 1$	$W_1[0, 12, 0, 11, 5] = 1$
$W_1[0, 12, 1, 0, 7] = 1$	$W_1[0, 12, 1, 7, 0] = 1$	$W_1[0, 12, 2, 0, 8] = 1$
$W_1[0, 12, 2, 8, 0] = 1$	$W_1[0, 12, 3, 0, 9] = 1$	$W_1[0, 12, 3, 9, 0] = 1$
$W_1[0, 12, 4, 0, 10] = 1$	$W_1[0, 12, 4, 10, 0] = 1$	$W_1[0, 12, 5, 0, 11] = 1$
$W_1[0, 12, 5, 11, 0] = 1$	$W_1[0, 12, 6, 0, 0] = 2$	$W_1[0, 12, 7, 0, 1] = 1$
$W_1[0, 12, 7, 1, 0] = 1$	$W_1[0, 12, 8, 0, 2] = 1$	$W_1[0, 12, 8, 2, 0] = 1$
$W_1[0, 12, 9, 0, 3] = 1$	$W_1[0, 12, 9, 3, 0] = 1$	$W_1[0, 12, 10, 0, 4] = 1$
$W_1[0, 12, 10, 4, 0] = 1$	$W_1[0, 12, 11, 0, 5] = 1$	$W_1[0, 12, 11, 5, 0] = 1$
$W_1[1, 0, 1, 6, 12] = 1$	$W_1[1, 0, 1, 12, 6] = 1$	$W_1[1, 0, 6, 1, 12] = 1$
$W_1[1, 0, 6, 12, 1] = 1$	$W_1[1, 0, 12, 1, 6] = 1$	$W_1[1, 0, 12, 6, 1] = 1$
$W_1[1, 1, 0, 6, 12] = 1$	$W_1[1, 1, 0, 12, 6] = 1$	$W_1[1, 1, 1, 7, 12] = 2$
$W_1[1, 1, 1, 12, 7] = 2$	$W_1[1, 1, 2, 8, 12] = 1$	$W_1[1, 1, 2, 12, 8] = 1$
$W_1[1, 1, 3, 9, 12] = 1$	$W_1[1, 1, 3, 12, 9] = 1$	$W_1[1, 1, 4, 10, 12] = 1$
$W_1[1, 1, 4, 12, 10] = 1$	$W_1[1, 1, 5, 11, 12] = 1$	$W_1[1, 1, 5, 12, 11] = 1$
$W_1[1, 1, 6, 0, 12] = 1$	$W_1[1, 1, 6, 12, 0] = 1$	$W_1[1, 1, 7, 1, 12] = 2$
$W_1[1, 1, 7, 12, 1] = 2$	$W_1[1, 1, 8, 2, 12] = 1$	$W_1[1, 1, 8, 12, 2] = 1$
$W_1[1, 1, 9, 3, 12] = 1$	$W_1[1, 1, 9, 12, 3] = 1$	$W_1[1, 1, 10, 4, 12] = 1$
$W_1[1, 1, 10, 12, 4] = 1$	$W_1[1, 1, 11, 5, 12] = 1$	$W_1[1, 1, 11, 12, 5] = 1$
$W_1[1, 1, 12, 0, 6] = 1$	$W_1[1, 1, 12, 1, 7] = 2$	$W_1[1, 1, 12, 2, 8] = 1$
$W_1[1, 1, 12, 3, 9] = 1$	$W_1[1, 1, 12, 4, 10] = 1$	$W_1[1, 1, 12, 5, 11] = 1$
$W_1[1, 1, 12, 6, 0] = 1$	$W_1[1, 1, 12, 7, 1] = 2$	$W_1[1, 1, 12, 8, 2] = 1$
$W_1[1, 1, 12, 9, 3] = 1$	$W_1[1, 1, 12, 10, 4] = 1$	$W_1[1, 1, 12, 11, 5] = 1$
$W_1[1, 2, 1, 8, 12] = 1$	$W_1[1, 2, 1, 12, 8] = 1$	$W_1[1, 2, 8, 1, 12] = 1$
$W_1[1, 2, 8, 12, 1] = 1$	$W_1[1, 2, 12, 1, 8] = 1$	$W_1[1, 2, 12, 8, 1] = 1$

TABLE IX. (*Continued.*)

$W_1[1, 3, 1, 9, 12] = 1$	$W_1[1, 3, 1, 12, 9] = 1$	$W_1[1, 3, 9, 1, 12] = 1$
$W_1[1, 3, 9, 12, 1] = 1$	$W_1[1, 3, 12, 1, 9] = 1$	$W_1[1, 3, 12, 9, 1] = 1$
$W_1[1, 4, 1, 10, 12] = 1$	$W_1[1, 4, 1, 12, 10] = 1$	$W_1[1, 4, 10, 1, 12] = 1$
$W_1[1, 4, 10, 12, 1] = 1$	$W_1[1, 4, 12, 1, 10] = 1$	$W_1[1, 4, 12, 10, 1] = 1$
$W_1[1, 5, 1, 11, 12] = 1$	$W_1[1, 5, 1, 12, 11] = 1$	$W_1[1, 5, 11, 1, 12] = 1$
$W_1[1, 5, 11, 12, 1] = 1$	$W_1[1, 5, 12, 1, 11] = 1$	$W_1[1, 5, 12, 11, 1] = 1$
$W_1[1, 6, 0, 1, 12] = 1$	$W_1[1, 6, 0, 12, 1] = 1$	$W_1[1, 6, 1, 0, 12] = 1$
$W_1[1, 6, 1, 12, 0] = 1$	$W_1[1, 6, 12, 0, 1] = 1$	$W_1[1, 6, 12, 1, 0] = 1$
$W_1[1, 7, 1, 1, 12] = 2$	$W_1[1, 7, 1, 12, 1] = 2$	$W_1[1, 7, 12, 1, 1] = 2$
$W_1[1, 8, 1, 2, 12] = 1$	$W_1[1, 8, 1, 12, 2] = 1$	$W_1[1, 8, 2, 1, 12] = 1$
$W_1[1, 8, 2, 12, 1] = 1$	$W_1[1, 8, 12, 1, 2] = 1$	$W_1[1, 8, 12, 2, 1] = 1$
$W_1[1, 9, 1, 3, 12] = 1$	$W_1[1, 9, 1, 12, 3] = 1$	$W_1[1, 9, 3, 1, 12] = 1$
$W_1[1, 9, 3, 12, 1] = 1$	$W_1[1, 9, 12, 1, 3] = 1$	$W_1[1, 9, 12, 3, 1] = 1$
$W_1[1, 10, 1, 4, 12] = 1$	$W_1[1, 10, 1, 12, 4] = 1$	$W_1[1, 10, 4, 1, 12] = 1$
$W_1[1, 10, 4, 12, 1] = 1$	$W_1[1, 10, 12, 1, 4] = 1$	$W_1[1, 10, 12, 4, 1] = 1$
$W_1[1, 11, 1, 5, 12] = 1$	$W_1[1, 11, 1, 12, 5] = 1$	$W_1[1, 11, 5, 1, 12] = 1$
$W_1[1, 11, 5, 12, 1] = 1$	$W_1[1, 11, 12, 1, 5] = 1$	$W_1[1, 11, 12, 5, 1] = 1$
$W_1[1, 12, 0, 1, 6] = 1$	$W_1[1, 12, 0, 6, 1] = 1$	$W_1[1, 12, 1, 0, 6] = 1$
$W_1[1, 12, 1, 1, 7] = 2$	$W_1[1, 12, 1, 2, 8] = 1$	$W_1[1, 12, 1, 3, 9] = 1$
$W_1[1, 12, 1, 4, 10] = 1$	$W_1[1, 12, 1, 5, 11] = 1$	$W_1[1, 12, 1, 6, 0] = 1$
$W_1[1, 12, 1, 7, 1] = 2$	$W_1[1, 12, 1, 8, 2] = 1$	$W_1[1, 12, 1, 9, 3] = 1$
$W_1[1, 12, 1, 10, 4] = 1$	$W_1[1, 12, 1, 11, 5] = 1$	$W_1[1, 12, 2, 1, 8] = 1$
$W_1[1, 12, 2, 8, 1] = 1$	$W_1[1, 12, 3, 1, 9] = 1$	$W_1[1, 12, 3, 9, 1] = 1$
$W_1[1, 12, 4, 1, 10] = 1$	$W_1[1, 12, 4, 10, 1] = 1$	$W_1[1, 12, 5, 1, 11] = 1$
$W_1[1, 12, 5, 11, 1] = 1$	$W_1[1, 12, 6, 0, 1] = 1$	$W_1[1, 12, 6, 1, 0] = 1$
$W_1[1, 12, 7, 1, 1] = 2$	$W_1[1, 12, 8, 1, 2] = 1$	$W_1[1, 12, 8, 2, 1] = 1$
$W_1[1, 12, 9, 1, 3] = 1$	$W_1[1, 12, 9, 3, 1] = 1$	$W_1[1, 12, 10, 1, 4] = 1$
$W_1[1, 12, 10, 4, 1] = 1$	$W_1[1, 12, 11, 1, 5] = 1$	$W_1[1, 12, 11, 5, 1] = 1$
$W_1[2, 0, 2, 6, 12] = 1$	$W_1[2, 0, 2, 12, 6] = 1$	$W_1[2, 0, 6, 2, 12] = 1$
$W_1[2, 0, 6, 12, 2] = 1$	$W_1[2, 0, 12, 2, 6] = 1$	$W_1[2, 0, 12, 6, 2] = 1$
$W_1[2, 1, 2, 7, 12] = 1$	$W_1[2, 1, 2, 12, 7] = 1$	$W_1[2, 1, 7, 2, 12] = 1$
$W_1[2, 1, 7, 12, 2] = 1$	$W_1[2, 1, 12, 2, 7] = 1$	$W_1[2, 1, 12, 7, 2] = 1$
$W_1[2, 2, 0, 6, 12] = 1$	$W_1[2, 2, 0, 12, 6] = 1$	$W_1[2, 2, 1, 7, 12] = 1$
$W_1[2, 2, 1, 12, 7] = 1$	$W_1[2, 2, 2, 8, 12] = 2$	$W_1[2, 2, 2, 12, 8] = 2$
$W_1[2, 2, 3, 9, 12] = 1$	$W_1[2, 2, 3, 12, 9] = 1$	$W_1[2, 2, 4, 10, 12] = 1$
$W_1[2, 2, 4, 12, 10] = 1$	$W_1[2, 2, 5, 11, 12] = 1$	$W_1[2, 2, 5, 12, 11] = 1$
$W_1[2, 2, 6, 0, 12] = 1$	$W_1[2, 2, 6, 12, 0] = 1$	$W_1[2, 2, 7, 1, 12] = 1$
$W_1[2, 2, 7, 12, 1] = 1$	$W_1[2, 2, 8, 2, 12] = 2$	$W_1[2, 2, 8, 12, 2] = 2$
$W_1[2, 2, 9, 3, 12] = 1$	$W_1[2, 2, 9, 12, 3] = 1$	$W_1[2, 2, 10, 4, 12] = 1$
$W_1[2, 2, 10, 12, 4] = 1$	$W_1[2, 2, 11, 5, 12] = 1$	$W_1[2, 2, 11, 12, 5] = 1$
$W_1[2, 2, 12, 0, 6] = 1$	$W_1[2, 2, 12, 1, 7] = 1$	$W_1[2, 2, 12, 2, 8] = 2$
$W_1[2, 2, 12, 3, 9] = 1$	$W_1[2, 2, 12, 4, 10] = 1$	$W_1[2, 2, 12, 5, 11] = 1$
$W_1[2, 2, 12, 6, 0] = 1$	$W_1[2, 2, 12, 7, 1] = 1$	$W_1[2, 2, 12, 8, 2] = 2$
$W_1[2, 2, 12, 9, 3] = 1$	$W_1[2, 2, 12, 10, 4] = 1$	$W_1[2, 2, 12, 11, 5] = 1$
$W_1[2, 3, 2, 9, 12] = 1$	$W_1[2, 3, 2, 12, 9] = 1$	$W_1[2, 3, 9, 2, 12] = 1$
$W_1[2, 3, 9, 12, 2] = 1$	$W_1[2, 3, 12, 2, 9] = 1$	$W_1[2, 3, 12, 9, 2] = 1$
$W_1[2, 4, 2, 10, 12] = 1$	$W_1[2, 4, 2, 12, 10] = 1$	$W_1[2, 4, 10, 2, 12] = 1$
$W_1[2, 4, 10, 12, 2] = 1$	$W_1[2, 4, 12, 2, 10] = 1$	$W_1[2, 4, 12, 10, 2] = 1$
$W_1[2, 5, 2, 11, 12] = 1$	$W_1[2, 5, 2, 12, 11] = 1$	$W_1[2, 5, 11, 2, 12] = 1$
$W_1[2, 5, 11, 12, 2] = 1$	$W_1[2, 5, 12, 2, 11] = 1$	$W_1[2, 5, 12, 11, 2] = 1$
$W_1[2, 6, 0, 2, 12] = 1$	$W_1[2, 6, 0, 12, 2] = 1$	$W_1[2, 6, 2, 0, 12] = 1$
$W_1[2, 6, 2, 12, 0] = 1$	$W_1[2, 6, 12, 0, 2] = 1$	$W_1[2, 6, 12, 2, 0] = 1$
$W_1[2, 7, 1, 2, 12] = 1$	$W_1[2, 7, 1, 12, 2] = 1$	$W_1[2, 7, 2, 1, 12] = 1$
$W_1[2, 7, 2, 12, 1] = 1$	$W_1[2, 7, 12, 1, 2] = 1$	$W_1[2, 7, 12, 2, 1] = 1$
$W_1[2, 8, 2, 2, 12] = 2$	$W_1[2, 8, 2, 12, 2] = 2$	$W_1[2, 8, 12, 2, 2] = 2$
$W_1[2, 9, 2, 3, 12] = 1$	$W_1[2, 9, 2, 12, 3] = 1$	$W_1[2, 9, 3, 2, 12] = 1$
$W_1[2, 9, 3, 12, 2] = 1$	$W_1[2, 9, 12, 2, 3] = 1$	$W_1[2, 9, 12, 3, 2] = 1$
$W_1[2, 10, 2, 4, 12] = 1$	$W_1[2, 10, 2, 12, 4] = 1$	$W_1[2, 10, 4, 2, 12] = 1$
$W_1[2, 10, 4, 12, 2] = 1$	$W_1[2, 10, 12, 2, 4] = 1$	$W_1[2, 10, 12, 4, 2] = 1$

TABLE IX. (*Continued.*)

$W_1[2, 11, 2, 5, 12] = 1$	$W_1[2, 11, 2, 12, 5] = 1$	$W_1[2, 11, 5, 2, 12] = 1$
$W_1[2, 11, 5, 12, 2] = 1$	$W_1[2, 11, 12, 2, 5] = 1$	$W_1[2, 11, 12, 5, 2] = 1$
$W_1[2, 12, 0, 2, 6] = 1$	$W_1[2, 12, 0, 6, 2] = 1$	$W_1[2, 12, 1, 2, 7] = 1$
$W_1[2, 12, 1, 7, 2] = 1$	$W_1[2, 12, 2, 0, 6] = 1$	$W_1[2, 12, 2, 1, 7] = 1$
$W_1[2, 12, 2, 2, 8] = 2$	$W_1[2, 12, 2, 3, 9] = 1$	$W_1[2, 12, 2, 4, 10] = 1$
$W_1[2, 12, 2, 5, 11] = 1$	$W_1[2, 12, 2, 6, 0] = 1$	$W_1[2, 12, 2, 7, 1] = 1$
$W_1[2, 12, 2, 8, 2] = 2$	$W_1[2, 12, 2, 9, 3] = 1$	$W_1[2, 12, 2, 10, 4] = 1$
$W_1[2, 12, 2, 11, 5] = 1$	$W_1[2, 12, 3, 2, 9] = 1$	$W_1[2, 12, 3, 9, 2] = 1$
$W_1[2, 12, 4, 2, 10] = 1$	$W_1[2, 12, 4, 10, 2] = 1$	$W_1[2, 12, 5, 2, 11] = 1$
$W_1[2, 12, 5, 11, 2] = 1$	$W_1[2, 12, 6, 0, 2] = 1$	$W_1[2, 12, 6, 2, 0] = 1$
$W_1[2, 12, 7, 1, 2] = 1$	$W_1[2, 12, 7, 2, 1] = 1$	$W_1[2, 12, 8, 2, 2] = 2$
$W_1[2, 12, 9, 2, 3] = 1$	$W_1[2, 12, 9, 3, 2] = 1$	$W_1[2, 12, 10, 2, 4] = 1$
$W_1[2, 12, 10, 4, 2] = 1$	$W_1[2, 12, 11, 2, 5] = 1$	$W_1[2, 12, 11, 5, 2] = 1$
$W_1[3, 0, 3, 6, 12] = 1$	$W_1[3, 0, 3, 12, 6] = 1$	$W_1[3, 0, 6, 3, 12] = 1$
$W_1[3, 0, 6, 12, 3] = 1$	$W_1[3, 0, 12, 3, 6] = 1$	$W_1[3, 0, 12, 6, 3] = 1$
$W_1[3, 1, 3, 7, 12] = 1$	$W_1[3, 1, 3, 12, 7] = 1$	$W_1[3, 1, 7, 3, 12] = 1$
$W_1[3, 1, 7, 12, 3] = 1$	$W_1[3, 1, 12, 3, 7] = 1$	$W_1[3, 1, 12, 7, 3] = 1$
$W_1[3, 2, 3, 8, 12] = 1$	$W_1[3, 2, 3, 12, 8] = 1$	$W_1[3, 2, 8, 3, 12] = 1$
$W_1[3, 2, 8, 12, 3] = 1$	$W_1[3, 2, 12, 3, 8] = 1$	$W_1[3, 2, 12, 8, 3] = 1$
$W_1[3, 3, 0, 6, 12] = 1$	$W_1[3, 3, 0, 12, 6] = 1$	$W_1[3, 3, 1, 7, 12] = 1$
$W_1[3, 3, 1, 12, 7] = 1$	$W_1[3, 3, 2, 8, 12] = 1$	$W_1[3, 3, 2, 12, 8] = 1$
$W_1[3, 3, 3, 9, 12] = 2$	$W_1[3, 3, 3, 12, 9] = 2$	$W_1[3, 3, 4, 10, 12] = 1$
$W_1[3, 3, 4, 12, 10] = 1$	$W_1[3, 3, 5, 11, 12] = 1$	$W_1[3, 3, 5, 12, 11] = 1$
$W_1[3, 3, 6, 0, 12] = 1$	$W_1[3, 3, 6, 12, 0] = 1$	$W_1[3, 3, 7, 1, 12] = 1$
$W_1[3, 3, 7, 12, 1] = 1$	$W_1[3, 3, 8, 2, 12] = 1$	$W_1[3, 3, 8, 12, 2] = 1$
$W_1[3, 3, 9, 3, 12] = 2$	$W_1[3, 3, 9, 12, 3] = 2$	$W_1[3, 3, 10, 4, 12] = 1$
$W_1[3, 3, 10, 12, 4] = 1$	$W_1[3, 3, 11, 5, 12] = 1$	$W_1[3, 3, 11, 12, 5] = 1$
$W_1[3, 3, 12, 0, 6] = 1$	$W_1[3, 3, 12, 1, 7] = 1$	$W_1[3, 3, 12, 2, 8] = 1$
$W_1[3, 3, 12, 3, 9] = 2$	$W_1[3, 3, 12, 4, 10] = 1$	$W_1[3, 3, 12, 5, 11] = 1$
$W_1[3, 3, 12, 6, 0] = 1$	$W_1[3, 3, 12, 7, 1] = 1$	$W_1[3, 3, 12, 8, 2] = 1$
$W_1[3, 3, 12, 9, 3] = 2$	$W_1[3, 3, 12, 10, 4] = 1$	$W_1[3, 3, 12, 11, 5] = 1$
$W_1[3, 4, 3, 10, 12] = 1$	$W_1[3, 4, 3, 12, 10] = 1$	$W_1[3, 4, 10, 3, 12] = 1$
$W_1[3, 4, 10, 12, 3] = 1$	$W_1[3, 4, 12, 3, 10] = 1$	$W_1[3, 4, 12, 10, 3] = 1$
$W_1[3, 5, 3, 11, 12] = 1$	$W_1[3, 5, 3, 12, 11] = 1$	$W_1[3, 5, 11, 3, 12] = 1$
$W_1[3, 5, 11, 12, 3] = 1$	$W_1[3, 5, 12, 3, 11] = 1$	$W_1[3, 5, 12, 11, 3] = 1$
$W_1[3, 6, 0, 3, 12] = 1$	$W_1[3, 6, 0, 12, 3] = 1$	$W_1[3, 6, 3, 0, 12] = 1$
$W_1[3, 6, 3, 12, 0] = 1$	$W_1[3, 6, 12, 0, 3] = 1$	$W_1[3, 6, 12, 3, 0] = 1$
$W_1[3, 7, 1, 3, 12] = 1$	$W_1[3, 7, 1, 12, 3] = 1$	$W_1[3, 7, 3, 1, 12] = 1$
$W_1[3, 7, 3, 12, 1] = 1$	$W_1[3, 7, 12, 1, 3] = 1$	$W_1[3, 7, 12, 3, 1] = 1$
$W_1[3, 8, 2, 3, 12] = 1$	$W_1[3, 8, 2, 12, 3] = 1$	$W_1[3, 8, 3, 2, 12] = 1$
$W_1[3, 8, 3, 12, 2] = 1$	$W_1[3, 8, 12, 2, 3] = 1$	$W_1[3, 8, 12, 3, 2] = 1$
$W_1[3, 9, 3, 3, 12] = 2$	$W_1[3, 9, 3, 12, 3] = 2$	$W_1[3, 9, 12, 3, 3] = 2$
$W_1[3, 10, 3, 4, 12] = 1$	$W_1[3, 10, 3, 12, 4] = 1$	$W_1[3, 10, 4, 3, 12] = 1$
$W_1[3, 10, 4, 12, 3] = 1$	$W_1[3, 10, 12, 3, 4] = 1$	$W_1[3, 10, 12, 4, 3] = 1$
$W_1[3, 11, 3, 5, 12] = 1$	$W_1[3, 11, 3, 12, 5] = 1$	$W_1[3, 11, 5, 3, 12] = 1$
$W_1[3, 11, 5, 12, 3] = 1$	$W_1[3, 11, 12, 3, 5] = 1$	$W_1[3, 11, 12, 5, 3] = 1$
$W_1[3, 12, 0, 3, 6] = 1$	$W_1[3, 12, 0, 6, 3] = 1$	$W_1[3, 12, 1, 3, 7] = 1$
$W_1[3, 12, 1, 7, 3] = 1$	$W_1[3, 12, 2, 3, 8] = 1$	$W_1[3, 12, 2, 8, 3] = 1$
$W_1[3, 12, 3, 0, 6] = 1$	$W_1[3, 12, 3, 1, 7] = 1$	$W_1[3, 12, 3, 2, 8] = 1$
$W_1[3, 12, 3, 3, 9] = 2$	$W_1[3, 12, 3, 4, 10] = 1$	$W_1[3, 12, 3, 5, 11] = 1$
$W_1[3, 12, 3, 6, 0] = 1$	$W_1[3, 12, 3, 7, 1] = 1$	$W_1[3, 12, 3, 8, 2] = 1$
$W_1[3, 12, 3, 9, 3] = 2$	$W_1[3, 12, 3, 10, 4] = 1$	$W_1[3, 12, 3, 11, 5] = 1$
$W_1[3, 12, 4, 3, 10] = 1$	$W_1[3, 12, 4, 10, 3] = 1$	$W_1[3, 12, 5, 3, 11] = 1$
$W_1[3, 12, 5, 11, 3] = 1$	$W_1[3, 12, 6, 0, 3] = 1$	$W_1[3, 12, 6, 3, 0] = 1$
$W_1[3, 12, 7, 1, 3] = 1$	$W_1[3, 12, 7, 3, 1] = 1$	$W_1[3, 12, 8, 2, 3] = 1$
$W_1[3, 12, 8, 3, 2] = 1$	$W_1[3, 12, 9, 3, 3] = 2$	$W_1[3, 12, 10, 3, 4] = 1$
$W_1[3, 12, 10, 4, 3] = 1$	$W_1[3, 12, 11, 3, 5] = 1$	$W_1[3, 12, 11, 5, 3] = 1$
$W_1[4, 0, 4, 6, 12] = 1$	$W_1[4, 0, 4, 12, 6] = 1$	$W_1[4, 0, 6, 4, 12] = 1$
$W_1[4, 0, 6, 12, 4] = 1$	$W_1[4, 0, 12, 4, 6] = 1$	$W_1[4, 0, 12, 6, 4] = 1$

TABLE IX. (*Continued.*)

$W_1[4, 1, 4, 7, 12] = 1$ $W_1[4, 1, 4, 12, 7] = 1$ $W_1[4, 1, 7, 4, 12] = 1$
$W_1[4, 1, 7, 12, 4] = 1$ $W_1[4, 1, 12, 4, 7] = 1$ $W_1[4, 1, 12, 7, 4] = 1$
$W_1[4, 2, 4, 8, 12] = 1$ $W_1[4, 2, 4, 12, 8] = 1$ $W_1[4, 2, 8, 4, 12] = 1$
$W_1[4, 2, 8, 12, 4] = 1$ $W_1[4, 2, 12, 4, 8] = 1$ $W_1[4, 2, 12, 8, 4] = 1$
$W_1[4, 3, 4, 9, 12] = 1$ $W_1[4, 3, 4, 12, 9] = 1$ $W_1[4, 3, 9, 4, 12] = 1$
$W_1[4, 3, 9, 12, 4] = 1$ $W_1[4, 3, 12, 4, 9] = 1$ $W_1[4, 3, 12, 9, 4] = 1$
$W_1[4, 4, 0, 6, 12] = 1$ $W_1[4, 4, 0, 12, 6] = 1$ $W_1[4, 4, 1, 7, 12] = 1$
$W_1[4, 4, 1, 12, 7] = 1$ $W_1[4, 4, 2, 8, 12] = 1$ $W_1[4, 4, 2, 12, 8] = 1$
$W_1[4, 4, 3, 9, 12] = 1$ $W_1[4, 4, 3, 12, 9] = 1$ $W_1[4, 4, 4, 10, 12] = 2$
$W_1[4, 4, 4, 12, 10] = 2$ $W_1[4, 4, 5, 11, 12] = 1$ $W_1[4, 4, 5, 12, 11] = 1$
$W_1[4, 4, 6, 0, 12] = 1$ $W_1[4, 4, 6, 12, 0] = 1$ $W_1[4, 4, 7, 1, 12] = 1$
$W_1[4, 4, 7, 12, 1] = 1$ $W_1[4, 4, 8, 2, 12] = 1$ $W_1[4, 4, 8, 12, 2] = 1$
$W_1[4, 4, 9, 3, 12] = 1$ $W_1[4, 4, 9, 12, 3] = 1$ $W_1[4, 4, 10, 4, 12] = 2$
$W_1[4, 4, 10, 12, 4] = 2$ $W_1[4, 4, 11, 5, 12] = 1$ $W_1[4, 4, 11, 12, 5] = 1$
$W_1[4, 4, 12, 0, 6] = 1$ $W_1[4, 4, 12, 1, 7] = 1$ $W_1[4, 4, 12, 2, 8] = 1$
$W_1[4, 4, 12, 3, 9] = 1$ $W_1[4, 4, 12, 4, 10] = 2$ $W_1[4, 4, 12, 5, 11] = 1$
$W_1[4, 4, 12, 6, 0] = 1$ $W_1[4, 4, 12, 7, 1] = 1$ $W_1[4, 4, 12, 8, 2] = 1$
$W_1[4, 4, 12, 9, 3] = 1$ $W_1[4, 4, 12, 10, 4] = 2$ $W_1[4, 4, 12, 11, 5] = 1$
$W_1[4, 5, 4, 11, 12] = 1$ $W_1[4, 5, 4, 12, 11] = 1$ $W_1[4, 5, 11, 4, 12] = 1$
$W_1[4, 5, 11, 12, 4] = 1$ $W_1[4, 5, 12, 4, 11] = 1$ $W_1[4, 5, 12, 11, 4] = 1$
$W_1[4, 6, 0, 4, 12] = 1$ $W_1[4, 6, 0, 12, 4] = 1$ $W_1[4, 6, 4, 0, 12] = 1$
$W_1[4, 6, 4, 12, 0] = 1$ $W_1[4, 6, 12, 0, 4] = 1$ $W_1[4, 6, 12, 4, 0] = 1$
$W_1[4, 7, 1, 4, 12] = 1$ $W_1[4, 7, 1, 12, 4] = 1$ $W_1[4, 7, 4, 1, 12] = 1$
$W_1[4, 7, 4, 12, 1] = 1$ $W_1[4, 7, 12, 1, 4] = 1$ $W_1[4, 7, 12, 4, 1] = 1$
$W_1[4, 8, 2, 4, 12] = 1$ $W_1[4, 8, 2, 12, 4] = 1$ $W_1[4, 8, 4, 2, 12] = 1$
$W_1[4, 8, 4, 12, 2] = 1$ $W_1[4, 8, 12, 2, 4] = 1$ $W_1[4, 8, 12, 4, 2] = 1$
$W_1[4, 9, 3, 4, 12] = 1$ $W_1[4, 9, 3, 12, 4] = 1$ $W_1[4, 9, 4, 3, 12] = 1$
$W_1[4, 9, 4, 12, 3] = 1$ $W_1[4, 9, 12, 3, 4] = 1$ $W_1[4, 9, 12, 4, 3] = 1$
$W_1[4, 10, 4, 4, 12] = 2$ $W_1[4, 10, 4, 12, 4] = 2$ $W_1[4, 10, 12, 4, 4] = 2$
$W_1[4, 11, 4, 5, 12] = 1$ $W_1[4, 11, 4, 12, 5] = 1$ $W_1[4, 11, 5, 4, 12] = 1$
$W_1[4, 11, 5, 12, 4] = 1$ $W_1[4, 11, 12, 4, 5] = 1$ $W_1[4, 11, 12, 5, 4] = 1$
$W_1[4, 12, 0, 4, 6] = 1$ $W_1[4, 12, 0, 6, 4] = 1$ $W_1[4, 12, 1, 4, 7] = 1$
$W_1[4, 12, 1, 7, 4] = 1$ $W_1[4, 12, 2, 4, 8] = 1$ $W_1[4, 12, 2, 8, 4] = 1$
$W_1[4, 12, 3, 4, 9] = 1$ $W_1[4, 12, 3, 9, 4] = 1$ $W_1[4, 12, 4, 0, 6] = 1$
$W_1[4, 12, 4, 1, 7] = 1$ $W_1[4, 12, 4, 2, 8] = 1$ $W_1[4, 12, 4, 3, 9] = 1$
$W_1[4, 12, 4, 4, 10] = 2$ $W_1[4, 12, 4, 5, 11] = 1$ $W_1[4, 12, 4, 6, 0] = 1$
$W_1[4, 12, 4, 7, 1] = 1$ $W_1[4, 12, 4, 8, 2] = 1$ $W_1[4, 12, 4, 9, 3] = 1$
$W_1[4, 12, 4, 10, 4] = 2$ $W_1[4, 12, 4, 11, 5] = 1$ $W_1[4, 12, 5, 4, 11] = 1$
$W_1[4, 12, 5, 11, 4] = 1$ $W_1[4, 12, 6, 0, 4] = 1$ $W_1[4, 12, 6, 4, 0] = 1$
$W_1[4, 12, 7, 1, 4] = 1$ $W_1[4, 12, 7, 4, 1] = 1$ $W_1[4, 12, 8, 2, 4] = 1$
$W_1[4, 12, 8, 4, 2] = 1$ $W_1[4, 12, 9, 3, 4] = 1$ $W_1[4, 12, 9, 4, 3] = 1$
$W_1[4, 12, 10, 4, 4] = 2$ $W_1[4, 12, 11, 4, 5] = 1$ $W_1[4, 12, 11, 5, 4] = 1$
$W_1[5, 0, 5, 6, 12] = 1$ $W_1[5, 0, 5, 12, 6] = 1$ $W_1[5, 0, 6, 5, 12] = 1$
$W_1[5, 0, 6, 12, 5] = 1$ $W_1[5, 0, 12, 5, 6] = 1$ $W_1[5, 0, 12, 6, 5] = 1$
$W_1[5, 1, 5, 7, 12] = 1$ $W_1[5, 1, 5, 12, 7] = 1$ $W_1[5, 1, 7, 5, 12] = 1$
$W_1[5, 1, 7, 12, 5] = 1$ $W_1[5, 1, 12, 5, 7] = 1$ $W_1[5, 1, 12, 7, 5] = 1$
$W_1[5, 2, 5, 8, 12] = 1$ $W_1[5, 2, 5, 12, 8] = 1$ $W_1[5, 2, 8, 5, 12] = 1$
$W_1[5, 2, 8, 12, 5] = 1$ $W_1[5, 2, 12, 5, 8] = 1$ $W_1[5, 2, 12, 8, 5] = 1$
$W_1[5, 3, 5, 9, 12] = 1$ $W_1[5, 3, 5, 12, 9] = 1$ $W_1[5, 3, 9, 5, 12] = 1$
$W_1[5, 3, 9, 12, 5] = 1$ $W_1[5, 3, 12, 5, 9] = 1$ $W_1[5, 3, 12, 9, 5] = 1$
$W_1[5, 4, 5, 10, 12] = 1$ $W_1[5, 4, 5, 12, 10] = 1$ $W_1[5, 4, 10, 5, 12] = 1$
$W_1[5, 4, 10, 12, 5] = 1$ $W_1[5, 4, 12, 5, 10] = 1$ $W_1[5, 4, 12, 10, 5] = 1$
$W_1[5, 5, 0, 6, 12] = 1$ $W_1[5, 5, 0, 12, 6] = 1$ $W_1[5, 5, 1, 7, 12] = 1$
$W_1[5, 5, 1, 12, 7] = 1$ $W_1[5, 5, 2, 8, 12] = 1$ $W_1[5, 5, 2, 12, 8] = 1$
$W_1[5, 5, 3, 9, 12] = 1$ $W_1[5, 5, 3, 12, 9] = 1$ $W_1[5, 5, 4, 10, 12] = 1$
$W_1[5, 5, 4, 12, 10] = 1$ $W_1[5, 5, 5, 11, 12] = 2$ $W_1[5, 5, 5, 12, 11] = 2$
$W_1[5, 5, 6, 0, 12] = 1$ $W_1[5, 5, 6, 12, 0] = 1$ $W_1[5, 5, 7, 1, 12] = 1$
$W_1[5, 5, 7, 12, 1] = 1$ $W_1[5, 5, 8, 2, 12] = 1$ $W_1[5, 5, 8, 12, 2] = 1$
$W_1[5, 5, 9, 3, 12] = 1$ $W_1[5, 5, 9, 12, 3] = 1$ $W_1[5, 5, 10, 4, 12] = 1$

TABLE IX. (*Continued.*)

$W_1[5, 5, 10, 12, 4] = 1$	$W_1[5, 5, 11, 5, 12] = 2$	$W_1[5, 5, 11, 12, 5] = 2$
$W_1[5, 5, 12, 0, 6] = 1$	$W_1[5, 5, 12, 1, 7] = 1$	$W_1[5, 5, 12, 2, 8] = 1$
$W_1[5, 5, 12, 3, 9] = 1$	$W_1[5, 5, 12, 4, 10] = 1$	$W_1[5, 5, 12, 5, 11] = 2$
$W_1[5, 5, 12, 6, 0] = 1$	$W_1[5, 5, 12, 7, 1] = 1$	$W_1[5, 5, 12, 8, 2] = 1$
$W_1[5, 5, 12, 9, 3] = 1$	$W_1[5, 5, 12, 10, 4] = 1$	$W_1[5, 5, 12, 11, 5] = 2$
$W_1[5, 6, 0, 5, 12] = 1$	$W_1[5, 6, 0, 12, 5] = 1$	$W_1[5, 6, 5, 0, 12] = 1$
$W_1[5, 6, 5, 12, 0] = 1$	$W_1[5, 6, 12, 0, 5] = 1$	$W_1[5, 6, 12, 5, 0] = 1$
$W_1[5, 7, 1, 5, 12] = 1$	$W_1[5, 7, 1, 12, 5] = 1$	$W_1[5, 7, 5, 1, 12] = 1$
$W_1[5, 7, 5, 12, 1] = 1$	$W_1[5, 7, 12, 1, 5] = 1$	$W_1[5, 7, 12, 5, 1] = 1$
$W_1[5, 8, 2, 5, 12] = 1$	$W_1[5, 8, 2, 12, 5] = 1$	$W_1[5, 8, 5, 2, 12] = 1$
$W_1[5, 8, 5, 12, 2] = 1$	$W_1[5, 8, 12, 2, 5] = 1$	$W_1[5, 8, 12, 5, 2] = 1$
$W_1[5, 9, 3, 5, 12] = 1$	$W_1[5, 9, 3, 12, 5] = 1$	$W_1[5, 9, 5, 3, 12] = 1$
$W_1[5, 9, 5, 12, 3] = 1$	$W_1[5, 9, 12, 3, 5] = 1$	$W_1[5, 9, 12, 5, 3] = 1$
$W_1[5, 10, 4, 5, 12] = 1$	$W_1[5, 10, 4, 12, 5] = 1$	$W_1[5, 10, 5, 4, 12] = 1$
$W_1[5, 10, 5, 12, 4] = 1$	$W_1[5, 10, 12, 4, 5] = 1$	$W_1[5, 10, 12, 5, 4] = 1$
$W_1[5, 11, 5, 5, 12] = 2$	$W_1[5, 11, 5, 12, 5] = 2$	$W_1[5, 11, 12, 5, 5] = 2$
$W_1[5, 12, 0, 5, 6] = 1$	$W_1[5, 12, 0, 6, 5] = 1$	$W_1[5, 12, 1, 5, 7] = 1$
$W_1[5, 12, 1, 7, 5] = 1$	$W_1[5, 12, 2, 5, 8] = 1$	$W_1[5, 12, 2, 8, 5] = 1$
$W_1[5, 12, 3, 5, 9] = 1$	$W_1[5, 12, 3, 9, 5] = 1$	$W_1[5, 12, 4, 5, 10] = 1$
$W_1[5, 12, 4, 10, 5] = 1$	$W_1[5, 12, 5, 0, 6] = 1$	$W_1[5, 12, 5, 1, 7] = 1$
$W_1[5, 12, 5, 2, 8] = 1$	$W_1[5, 12, 5, 3, 9] = 1$	$W_1[5, 12, 5, 4, 10] = 1$
$W_1[5, 12, 5, 5, 11] = 2$	$W_1[5, 12, 5, 6, 0] = 1$	$W_1[5, 12, 5, 7, 1] = 1$
$W_1[5, 12, 5, 8, 2] = 1$	$W_1[5, 12, 5, 9, 3] = 1$	$W_1[5, 12, 5, 10, 4] = 1$
$W_1[5, 12, 5, 11, 5] = 2$	$W_1[5, 12, 6, 0, 5] = 1$	$W_1[5, 12, 6, 5, 0] = 1$
$W_1[5, 12, 7, 1, 5] = 1$	$W_1[5, 12, 7, 5, 1] = 1$	$W_1[5, 12, 8, 2, 5] = 1$
$W_1[5, 12, 8, 5, 2] = 1$	$W_1[5, 12, 9, 3, 5] = 1$	$W_1[5, 12, 9, 5, 3] = 1$
$W_1[5, 12, 10, 4, 5] = 1$	$W_1[5, 12, 10, 5, 4] = 1$	$W_1[5, 12, 11, 5, 5] = 2$

the physical variable (varying from 0 to 5), with weights $(1, 0, -1)$, $(1, -1, 1)$, $(0, -1, 0)$, $(0, 1, 0)$, $(-1, 1, -1)$, and $(-1, 0, 1)$, respectively. The four subsequent indices the virtual variables on the links (in, e.g., clockwise direction). For X_{31}, this corresponds to the virtual space $\mathcal{V} = \mathbf{4} \oplus \overline{\mathbf{4}}$ with weights $(1, 0, 0)$, $(-1, 1, 0)$, $(0, -1, 1)$, $(0, 0, -1)$, $(-1, 0, 0)$, $(1, -1, 0)$, $(0, 1, -1)$ and $(0, 0, 1)$. For W_1, this corresponds to the SU(6) virtual space $\mathcal{V} = \mathbf{6} \oplus \overline{\mathbf{6}} \oplus \mathbf{1}$, with weights $(1,0,0,0,0)$, $(-1, 1, 0, 0, 0)$, $(0, -1, 1, 0, 0)$, $(0, 0, -1, 1, 0)$, $(0, 0, 0, -1, 1)$, $(0, 0, 0, 0, -1)$, $(-1, 0, 0, 0, 0)$, $(1, -1, 0, 0, 0)$, $(0, 1, -1, 0, 0)$, $(0, 0, 1, -1, 0)$, $(0, 0, 0, 1, -1)$, $(0,0,0,0,1)$, and $(0,0,0,0,0)$.

[1] M. A. Cazalilla and A. M. Rey, Ultracold Fermi gases with emergent SU(*N*) symmetry, Rep. Prog. Phys. **77**, 124401 (2014).

[2] C. Hofrichter, L. Riegger, F. Scazza, M. Hfer, D. R. Fernandes, I. Bloch, and S. Flling, Direct Probing of the Mott Crossover in the SU(*N*) Fermi-Hubbard Model, Phys. Rev. X **6**, 021030 (2016).

[3] B. Sutherland, Model for a multicomponent quantum system, Phys. Rev. B **12**, 3795 (1975).

[4] N. Read and S. Sachdev, Some features of the phase diagram of the square lattice SU(*N*) antiferromagnet, Nucl. Phys. B **316**, 609 (1989).

[5] N. Read and S. Sachdev, Spin-Peierls, valence-bond solid, and Néel ground states of low-dimensional quantum antiferromagnets, Phys. Rev. B **42**, 4568 (1990).

[6] P. Corboz, A. M. Läuchli, K. Penc, M. Troyer, and F. Mila, Simultaneous Dimerization and SU(4) Symmetry Breaking of 4-Color Fermions on the Square Lattice, Phys. Rev. Lett. **107**, 215301 (2011).

[7] B. Bauer, P. Corboz, A. M. Läuchli, L. Messio, K. Penc, M. Troyer, and F. Mila, Three-sublattice order in the SU(3) Heisenberg model on the square and triangular lattice, Phys. Rev. B **85**, 125116 (2012).

[8] S. Capponi, P. Lecheminant, and K. Totsuka, Phases of one-dimensional SU(*N*) cold atomic Fermi gases—From molecular Luttinger liquids to topological phases, Ann. Phys. **367**, 50 (2016).

[9] O. Gauthé and D. Poilblanc, Entanglement properties of the two-dimensional SU(3) Affleck-Kennedy-Lieb-Tasaki state, Phys. Rev. B **96**, 121115(R) (2017).

[10] X.-Y. Dong, J.-Y. Chen, and H.-H. Tu, SU(3) trimer resonating-valence-bond state on the square lattice, Phys. Rev. B **98**, 205117 (2018).

[11] I. Kurečić, L. Vanderstraeten, and N. Schuch, Gapped SU(3) spin liquid with $\mathbb{Z}_3$ topological order, Phys. Rev. B **99**, 045116 (2019).

[12] F. F. Assaad, Phase diagram of the half-filled two-dimensional SU(*N*) Hubbard-Heisenberg model: A quantum Monte Carlo study, Phys. Rev. B **71**, 075103 (2005).

[13] F. H. Kim, K. Penc, P. Nataf, and F. Mila, Linear flavor-wave theory for fully antisymmetric SU(N) irreducible representations, Phys. Rev. B **96**, 205142 (2017).

[14] F. H. Kim, F. F. Assaad, K. Penc, and F. Mila, Dimensional crossover in the SU(4) Heisenberg model in the six-dimensional antisymmetric self-conjugate representation revealed by quantum Monte Carlo and linear flavor-wave theory, Phys. Rev. B **100**, 085103 (2019).

[15] I. Affleck, D. P. Arovas, J. B. Marston, and D. A. Rabson, SU($2n$) quantum antiferromagnets with exact $\mathcal{C}$-breaking ground states, Nucl. Phys. B **366**, 467 (1991).

[16] A. Paramekanti and J. B. Marston, SU(N) quantum spin models: A variational wave function study, J. Phys.: Condens. Matter **19**, 125215 (2007).

[17] D. Wang, Y. Li, Z. Cai, Z. Zhou, Y. Wang, and C. Wu, Competing Orders in the 2D Half-Filled SU($2N$) Hubbard Model Through the Pinning-Field Quantum Monte Carlo Simulations, Phys. Rev. Lett. **112**, 156403 (2014).

[18] K. Harada, N. Kawashima, and M. Troyer, Néel and Spin-Peierls Ground States of Two-Dimensional SU(N) Quantum Antiferromagnets, Phys. Rev. Lett. **90**, 117203 (2003).

[19] O. Gauthé, S. Capponi, and D. Poilblanc, SU(4) topological resonating valence bond spin liquid on the square lattice, Phys. Rev. B **99**, 241112(R) (2019).

[20] In fact, the pairs of nearest-neighbor virtual states are projected onto SU(4) singlets. This is enforced by inserting matrices on the bond centers. Examples of PEPS are shown in Figs. 3(b) and 3(c).

[21] M. Mambrini, R. Orús, and D. Poilblanc, Systematic construction of spin liquids on the square lattice from tensor networks with SU(2) symmetry, Phys. Rev. B **94**, 205124 (2016).

[22] F. Pollmann, J. J. Betouras, K. Shtengel, and P. Fulde, Fermionic quantum dimer and fully packed loop models on the square lattice, Phys. Rev. B **83**, 155117 (2011).

[23] D. Poilblanc, M. Mambrini, and S. Capponi, Critical colored-RVB states in the frustrated quantum Heisenberg model on the square lattice, SciPost Phys. **7**, 041 (2019).

[24] For DMRG, we have computed the ground-state wave function on several cylinders $L_x \times L_y$ (with $L_x = 2L_y$) with open/periodic boundary conditions in the long/short direction. We have used explicitly the three U(1) quantum numbers to ease convergence and obtain the average ground-state energy per site e_0 as twice the total energy divided by the number of bonds. Using up to $m = 4000$ states, we can obtain reliable energies up to $L_y = 5$ or 6 depending on the value of θ. Moreover, assuming a small dependence with L_x, each data point is a variational energy for a fixed L_y. Our calculations have been implemented using the ITensor C++ library, available at http://itensor.org.

[25] P. Calabrese and J. Cardy, Entanglement entropy and quantum field theory, J. Stat. Mech.: Theory Exp. (2004) P06002 .

[26] P. Corboz, P. Czarnik, G. Kapteijns, and L. Tagliacozzo, Finite Correlation Length Scaling with Infinite Projected Entangled-Pair States, Phys. Rev. X **8**, 031031 (2018).

[27] S. V. Isakov, P. Fendley, A. W. W. Ludwig, S. Trebst, and M. Troyer, Dynamics at and near conformal quantum critical points, Phys. Rev. B **83**, 125114 (2011).

[28] G. Pagano, M. Mancini, G. Cappellini, P. Lombardi, F. Schäfer, H. Hu, X.-J. Liu, J. Catani, C. Sias, M. Inguscio, and L. Fallani, A one-dimensional liquid of fermions with tunable spin, Nat. Phys. **10**, 198 (2014).

[29] P. Nataf and F. Mila, Exact Diagonalization of Heisenberg SU(N) Models, Phys. Rev. Lett. **113**, 127204 (2014).

[30] Ji-Yao Chen, S. Capponi, A. Wietek, M. Mambrini, N. Schuch, and D. Poilblanc, SU(3)$_1$ chiral spin liquid on the square lattice: A view from symmetric PEPS, arXiv:1912.13393.